Historic, archived document

Do not assume content reflects current
scientific knowledge, policies, or practices.

STA/STA

United States
Department of
Agriculture

Forest Service

Intermountain
Forest and Range
Experiment Station
Ogden, UT 84401

Research Paper
INT-289

June 1982

A Reexamination of Fire Spread in Free-Burning Porous Fuel Beds

Ralph A. Wilson, Jr.

RESEARCH SUMMARY

The original assumption (made by Rothermel in his 1972 paper—A Mathematical Model for Predicting Fire Spread in Wildland Fuels) that the reaction intensity in the combustion zone is linear with loading is experimentally supported within the fuel sizes, loadings, and packing ratios commonly encountered in wildland fuels; further confirmation is needed in light loadings of the fine fuels.

Rothermel's empirical relations for the propagating flux ratio are judged to be adequate for their current use, though perhaps they underestimate the propagating flux in heavy loads of fine fuels. New evidence is presented to physically relate the propagating flux ratio to the optical density ($\sigma\beta$) of the fuel bed. Again, further development is needed.

Experimental difficulties in rigorous determination of reaction zone size remain unsolved. Thus, physical interpretation of reaction intensities should be made with caution. Similarly, the causes and consequences of the optimum packing ratio should be interpreted with caution; for example (in the author's opinion), the idea that reaction intensity is limited by oxygen supply (in draft) at heavier packing ratios is premature and has been overemphasized.

THE AUTHOR

RALPH A. WILSON, JR., is a research physicist assigned to the Fire Behavior research work unit at the Northern Forest Fire Laboratory, Missoula, Mont. His undergraduate studies were at Willamette University, Salem, Oreg., (B.A. 1956) with graduate work from 1956 to 1960 at University of Oregon (M.A. 1958). He worked in infrared detectors and optics at Naval Ordnance Test Station, China Lake, Calif., from 1957 to 1964. He then joined the Forest Service's airborne infrared forest fire surveillance project at Northern Forest Fire Laboratory, working as project scientist until 1975.

CONTENTS

Page

Introduction 1
Preliminary Discussion 1
Fire Model Geometric Equations 2
Moisture Damping 2
Experimental Setup 4
  Spread Rate 10
  Reaction Intensity 10
  Flame Depth / Residence Time 10
  Flame Height 13
  Index of Marginal Burning 13
DISCUSSION OF RESULTS 13
  Reaction Intensity, Reaction Velocity 13
  Propagating Flux Ratio 14
  Fuel Moisture 14
  Extinction 20
Summary 20
Publications Cited 21
Appendix — Tabulated Experimental Data 21

United States
Department of
Agriculture

Forest Service

**Intermountain
Forest and Range
Experiment Station
Ogden, UT 84401**

Research Paper
INT-289

June 1982

A Reexamination of Fire Spread in Free-Burning Porous Fuel Beds

Ralph A. Wilson, Jr.

INTRODUCTION

A mathematical model for fire in wildland fuels (Rothermel 1972) is the basis of several forest fire management systems. During development of the model, Rothermel found it necessary to make several assumptions about the effects of fuel geometry and fuel moisture upon combustion. The experimental work described here was initiated to examine these assumptions and to extend the data base beyond the range of Rothermel's early work. The interactions between fuel moisture, load, depth, packing ratio, and fuel particle size are of primary concern, because some combinations of these variables represent fuel arrays that will not support fire. We consider only the no-wind and zero-slope case.

Analysis of data from more than 250 experimental fires indicates clearly that additional data (probably 100 fires) are needed before definitive corrections can be made to the fire model equations. Although the results presented here are preliminary and tentative, some of the original assumptions are confirmed: the original functional form of the spread equations is retained for the geometric variables (σ, β, δ, w_o, etc.) while the numerical coefficients are reevaluated; a simplified fuel moisture-damping coefficient is proposed; a separate probability function is introduced to predict extinguishment. Reaction and critique are solicited.

PRELIMINARY DISCUSSION

Following the lead of Frandsen (1971), Rothermel (1972) developed the basic spread rate equations based on physical principles. One can begin with the proposition that the propagating flux (I_p) required to drive a fire is proportional to the heat needed to bring the fuel to ignition ($\rho_b \varepsilon Q_{ig}$);[1]

$$I_p = R(\rho_b \varepsilon Q_{ig}) \quad (1)$$

where the constant of proportionality is the spread rate, R. The preignition term ($\rho_b \varepsilon Q_{ig}$) is experimentally determined by calorimetric methods and is not considered here. The propagating flux is dependent on the fuel particle size, arrangement, chemistry, and environmental variables.

We next postulate that the propagating flux is proportional to the reaction intensity, I_R (the power density released by the fire),

$$I_p = \xi I_R \quad (2)$$

and assume that ξ is a function of only fuel bed geometry (i.e., the fraction of energy transferred to the fuel is a function of particle size and packing ratio, etc.).

An important key to Rothermel's success is the concept of independently evaluating I_p and I_R so that spread rate can be functionally related to the reaction intensity defined by:

$$I_R = -h\,(dw/dt). \quad (3)$$

Then by a series of definitions and logical assumptions the reaction intensity (Rothermel's equation 27) becomes a product of mathematically separable functions of the primary independent variables (σ, β, δ, w_o, M_f, etc.)

$$I_R = w_n\, h\, \Gamma'\, \eta_M\, \eta_S \quad (4)$$

In summary, it has been assumed (heretofore) that

- The propagation flux, I_p, is linearly proportional to reaction intensity, I_R;
- The proportionality constant, ξ, depends only on fuel particle size and fuel bed packing ratio;
- I_R is linearly proportional to net loading, w_n;
- The moisture-damping coefficient, η_M, is a function of fuel moisture, M_f, alone;
- The mineral-damping coefficient, η_S, depends only on the silica-free mineral content of the fuel; and
- Optimum reaction velocity (the average net fractional dry weight loss rate in the combustion zone) is a function of packing ratio only for fuel beds with only one size of fuel particle, σ.

[1] The nomenclature is defined in table 1, "Basic Fire Spread Equations," reproduced in metric form from p. 26, 27, Rothermel's paper and Wilson (1980).

Furthermore, the empirical damping coefficients, η_M and η_S, are defined such that

- $\eta_M = 1$ at $M_f = 0$ and
- $\eta_s = 1$ at $S_e = 0$; thus,
- $I_R = w_n h \Gamma'$ properly describes the fire state in the limit of no fuel moisture and no minerals.

As shown below, the experimentally determined reaction intensity, I_R, is dependent on the experimentally determined reaction zone size, and the propagating flux ratio, ξ, is determined as the fraction of I_R that is required to drive the fire at the measured spread rate, R. Thus, any consistent experimental technique for determining the reaction intensity will provide a consistent set of equations for I_R and ξ that will predict the spread rate, R (within the range of experimental applicability). The reaction intensity, however, is also used in applied models to predict other fire phenomena such as total heat release, flame length, scorch height, and fireline intensity. The reaction intensity, per se, is not derived from compensating factors and must represent as accurately as possible what it is purported to be. So, the experimental method of determining reaction zone size and hence reaction intensity must be carefully defined. In specific applications, the experimental method of determining "reaction intensity" may be significant for predicting specific fire phenomena.

FIRE MODEL GEOMETRIC EQUATIONS

Analysis of the geometric variables, σ, β, and δ, are confined to tests of the original fire equations against the expanded data base. The new data are restricted to the case of no wind, zero (level) slope, and a minimum of variation in fuel chemistry.

Rothermel's equations are reduced to a factor-product form for testing against the new data by the following substitutions in equations 27, 36, 37, and 38 of table 1.[2]

$$C_1 = \ln\left(\frac{\rho_p h \eta_S \Gamma'_{max}(1 - S_t)}{100}\right) + A(1 - \ln(\beta_{op}))$$

$$C_2 = A + 1$$

$$C_3 = -A/\beta_{op}.$$

A fourth parameter, C_4, is introduced to test the linearity of reaction intensity with loading and note that in the original formulation $C_4 = 1$.

The reaction intensity equation becomes

$$I_R = -h\left(\frac{dw}{dt}\right) = e^{C_1} \beta^{C_2} e^{C_3\beta} \delta^{C_4} \eta_M \qquad (5)$$

where the C_i coefficients are dependent on fuel size, σ, alone. Anticipating a linear regression technique, the log transform of equation 5 is:

$$\ln(I_R) = C_1 + C_2 \ln(\beta) + C_3\beta + C_4 \ln(\delta) + \ln(\eta_M). \qquad (6)$$

Note that in the ovendry limit $\eta_M = 1$ (also that in Rothermel's equations $C_4 = 1$). Evaluation of the coefficients by least square error fit and comparison with the original values will test the fire model formulation.

Similarly, the reaction velocity, Γ', becomes

$$\Gamma' = \left(\frac{100\, e^{C_1}}{\rho_p \quad \eta_M \quad \eta_S}\right) \beta^{C_2 - 1} e^{C_3\beta} \delta^{C_4 - 1}. \qquad (7)$$

The optimum packing ratio β_{op} is defined as the packing ratio at the maximum value of the reaction velocity.

Setting $\left.\frac{\partial \Gamma'}{\partial \beta}\right|_{\beta_{op}} = 0$

we have $\beta_{op} = (1 - C_2)/C_3$ (8)

whereby the optimum packing ratio is determined by the regression coefficients C_2 and C_3.

In similar fashion, the propagating flux ratio, ξ, is expressed as:

$$\xi = I_p/I_R = R(\rho_p \varepsilon Q_{ig}) / (-h\frac{dw}{dt}).$$

Again substituting coefficients in equation 42 of table 1:

$$d_1 = [0.0792 + 0.37597\, \sigma^{0.5} - \ln(192 + 7.9095\sigma)]$$

$$d_2 = [0.792 + 3.7597\sigma^{0.5}]$$

the propagating flux ratio becomes

$$\xi = \exp(d_1 + d_2\beta)$$

or

$$\ln(I_p/I_R) = d_1 + d_2\beta, \qquad (9)$$

where d_1 and d_2 are dependent on fuel particle size, σ.

Again, the coefficients, d_i, can be determined from the data and compared to Rothermel's original values.

In addition to the above, we introduce a dimensionless geometric parameter—the product, $\sigma\beta\delta$, which is the total surface area of all fuel particles per unit area of fuel bed. We note that heat transport out of the combustion zone, heat absorption by fuel particles, moisture mass transport into and out of fuels, production of volatile combustion products by pyrolysis, etc., are all related to fuel surface area (further theoretical consideration is beyond the scope of this paper). This product ($\sigma\beta\delta$) is used below in exploration of the limits of combustion.

The product ($\sigma\beta$) has the physical character of a radiation extinction coefficient and is introduced below in speculation concerning the propagating flux ratio.

MOISTURE DAMPING

The empirical form of the moisture damping coefficient, η_M, used by Rothermel is

$$\eta_M = \sum b_n \left(\frac{M_f}{M_x}\right)^n. \qquad (10)$$

This arbitrary power series was easily fitted to the limited data available and met the requirements that in the dry fuel limit

[2] Note: the factor (in the equation for C_1), 1/100, Is due to measurement of fuel bed depth in centimeters rather than meters.

Table 1.—Basic fire spread equations

Equations	Units and dimension	Equations (Rothermel 1972)
$R = \frac{I_R \xi (1 + \phi_w + \phi_s)}{\rho_b \varepsilon Q_{ig}}$	Rate of spread, m/min	(52)
$I_R = \Gamma' w_n h \eta_M \eta_s$	Reaction intensity, (kJ/min)/m^2	(27)

where:

$\Gamma' = \Gamma'_{max}(\beta/\beta_{op})^A \exp[A(1 - \beta/\beta_{op})]$	Optimum reaction velocity, min^{-1}	(38)
$\Gamma'_{max} = (0.0591 + 2.926\sigma^{-1.5})^{-1}$	Maximum reaction velocity, min^{-1}	(36)
$\beta_{op} = 0.204\sigma^{-0.8189}$	Optimum packing ratio	(37)
$A = (6.723\sigma^{0.1} - 7.27)$		(39)
$\eta_M = 1 - 2.59\left(\frac{M_f}{M_x}\right) + 5.11\left(\frac{M_f}{M_x}\right)^2 - 3.52\left(\frac{M_f}{M_x}\right)^3$	Moisture-damping coefficient	(29)
$\eta_s = 0.174 S_e^{-0.19}$	Mineral-damping coefficient	(30)
$\xi = (192 + 7.9095\sigma)^{-1} \exp[(0.792 + 3.760\sigma^{0.5})(\beta + 0.1)]$	Propagating flux ratio	(42)
$\phi_w = C(0.305U)^B \left(\frac{\beta}{\beta_{op}}\right)^{-E}$	Wind coefficient	(47)
$C = 7.47 \exp(-0.8711\sigma^{0.55})$		(48)
$B = 0.1599\sigma^{0.54}$		(49)
$E = 0.715\exp(-0.01094\sigma)$		(50)
$w_n = w_o(1 - S_T)$	Net fuel loading, kg/m^2	(24)
$\phi_s = 5.275\beta^{-0.3}(\tan\phi)^2$	Slope factor	(51)
$\rho_b = w_o/\delta$	Ovendry bulk density, kg/m^3	(40)
$\varepsilon = \exp(-4.528/\sigma)$	Effective heating number	(14)
$Q_{ig} = 581 + 2594M_f$	Heat of preignition, kJ/kg	(12)
$\beta = \frac{\rho_b}{\rho_p}$	Packing ratio	(31)

Input parameters for basic equations

w_o, ovendry fuel loading, kg/m^2

δ, fuel depth, m

σ, fuel particle surface-area-to-volume ratio, cm^{-1}

h, fuel particle low heat content, kJ/kg

ρ_p, ovendry particle density, kg/m^3

M_f, fuel particle moisture content, $\frac{\text{gm moisture}}{\text{gm ovendry wood}}$

S_T, fuel particle total mineral content, $\frac{\text{gm minerals}}{\text{gm ovendry wood}}$

S_e, fuel particle effective mineral content, $\frac{\text{gm silica-free minerals}}{\text{gm ovendry wood}}$

U, wind velocity at midflame height, m/min

tan ϕ, slope, vertical rise/horizontal distance

M_x, moisture content of extinction, dimensionless fraction

$\eta_M = 1$ at $M_f = 0$

and at the extinction limit of combustion

$\eta_M = 0$ at $M_f = M_x$.

The requirement that the moisture damping function also provides for extinguishment at the marginal limits of burning has not worked satisfactorily in application, primarily because we have been unable to find a consistent rationale for choosing a value of the moisture of extinction, M_x.

An alternative approach suggested here (and supported by analysis below) is to separate extinction from moisture damping. A separate probability function is proposed to predict the marginal burning state of the fire and then, if it will burn, a less complicated form of the damping coefficient is needed to characterize fuel moisture effects.

From among several alternatives, a good fit to the new data is given by

$$\eta_M = \exp(C_5 M_f) \quad (11)$$

which meets the only requirement that $\eta_M = 1$ at $M_f = 0$ for interpretation of the dry fuel limit in equation 5 above. Then regression equation 6 becomes

$$\ln(I_R) = C_1 + C_2 \ln(\beta) + C_3 \beta + C_4 \ln(\delta) + C_5 M_f. \quad (12)$$

The marginal burning probability function is discussed in the results section below. By this rationale the moisture damping function will characterize the effects of fuel moisture on I_R **of burning fires**; an independent function will predict the probability that it will burn or not burn.

EXPERIMENTAL SETUP

Three size classes of fuel were studied: *Populus* spp. (poplar) excelsior ($\sigma = 81.3\ cm^{-1}$); ponderosa pine, 1/4-inch-square sticks ($\sigma = 6.30\ cm^{-1}$); and ponderosa pine, 1/2-inch sticks ($\sigma = 3.5\ cm^{-1}$).

The fuels used in these experiments were chosen to minimize the effects of physiochemical variations (fuels chosen were high-cellulose, low-ash woods and were milled to precise dimensions). The physiochemical characteristics were determined by standard techniques and are tabulated in table 2.

A series of preliminary fires were burned to establish the range of fire phenomena over the experimental range of interest of fuel moisture and loading. These fires were also used to check out instrumentation and measurement techniques. Preliminary test results are given in appendix table 6.

Table 3 shows the matrix of variables examined. For scheduling and accounting purposes, a group number was assigned to each specific combination of σ, β, and δ such that for each fuel size, data would be obtained for a series of groups

- at one constant fuel depth for all packing ratios;
- at one constant packing ratio for all depths;
- at least one constant load for all depths; and,
- within practical limits, loadings and packing would be duplicated for the different fuel sizes.

Within each group (σ, β, δ), fires were burned at various fuel moisture contents from near ovendry up to $M_f = 0.30$. The moisture saturation limit of wood fiber is approximately 30 percent of the ovendry wood weight and is the upper limit of woody fuels ability to absorb moisture from the atmosphere without immersion in liquid water.

Fuels were prepared for a series of burns at a given fuel moisture content by conditioning at controlled temperature and relative humidity for 3 to 10 days, depending on fuel size and target fuel moisture. Prior to conditioning of the excelsior, the dry weight load corrected for storage equilibrium moisture content (EMC) for each burn was measured out into baskets. To construct the fuel bed, excelsior from the conditioning basket was spread uniformly over the bed, fluffed to 2 or 3 times the planned fuel depth to remove tightly packed concentrations, and lightly and uniformly pressed down to the final fuel depth (fig. 1A, B). Extraneous vertical strands above the bed surface were then clipped. Packing ratio for excelsior was calculated from $\beta = w_o / \rho\delta$.

The first 10 burns were loaded heavily (assuming $\rho = 32\ lb/ft^3$) before density measurements were completed from fuel samples.

For the larger pine fuels (1/4- and 1/2-inch-square sticks), the packing ratio was controlled directly by constructing each horizontal layer (4 or 2 layers per inch of depth, respectively) with the planned (solid volume/total volume) ratio (figs. 2, 3).

Raw data were collected by an automatic digital system (fig. 4) consisting of a programmable controller, clock, 80-channel scanner, digital multimeter, thermocouple reference junctions, digital weighing system, 35 mm camera, and associated interfaces and sensors. (Manual data acquisition consisted of visual measurements of the flame depth and flame height, a photograph of the fuel bed prior to ignition, and a tailing edge view of the fire.)

Table 2.—Physiochemical characteristics of fuels

Fuel	Surface/volume (σ), cm^{-1}	Particle density (ρ_p), kg/m^3	Heat of combustion (h), kJ/kg	Total mineral content (S_T), fraction	Effective mineral content (S_e), fraction
Excelsior (poplar)	81.3	466	17 550	0.00347	0.00322
1/4-inch sticks (ponderosa pine)	6.30	442	19 660	.00238	.00224
1/2-inch sticks (ponderosa pine)	3.15	444	19 163	.00367	.00322

Table 3.—Fuel loading matrix. First number is the I.D. index to identify a group of burns (series of fuel moistures) with constant loading and geometry. Second number is the (ovendry) fuel load in kg/m²

Fuel bed depth (cm)	Surface volume σ(cm^{-1})	Packing ratio, β						
		0.005	0.01	0.02	0.04	0.08	0.16	0.32
1.27	81.3		3, 0.050	*	9, 0.201			
	6.3							
	3.15							
2.54	81.3	1, 0.050	4, .101	8, 0.201	10, .402	11, 0.804		
	6.3				16, .448	20, .895	22, 1.790	
	3.15					27, .895		33, 3.580
5.08	81.3		5, .201	*	*			
	6.3		*	13, .448	17, .895	21, 1.790	23, 3.580	
	3.15					28, 1.790	31, 3.580	
10.16	81.3	2, .201	6, .402					
	6.3			14, .895	18, 1.790			
	3.15		*	24, .895	25, 1.790	29, 3.580	32, 7.161	34, 14.322
20.32	81.3		7, .804	*				
	6.3		12, .895	15, 1.790	19, 3.580			
	3.15				26, 3.580	30, 7.161		

*Indicated individual special purpose fires: to test the low moisture limit versus packing. etc. (labeled Group #0 in appendix table 5).

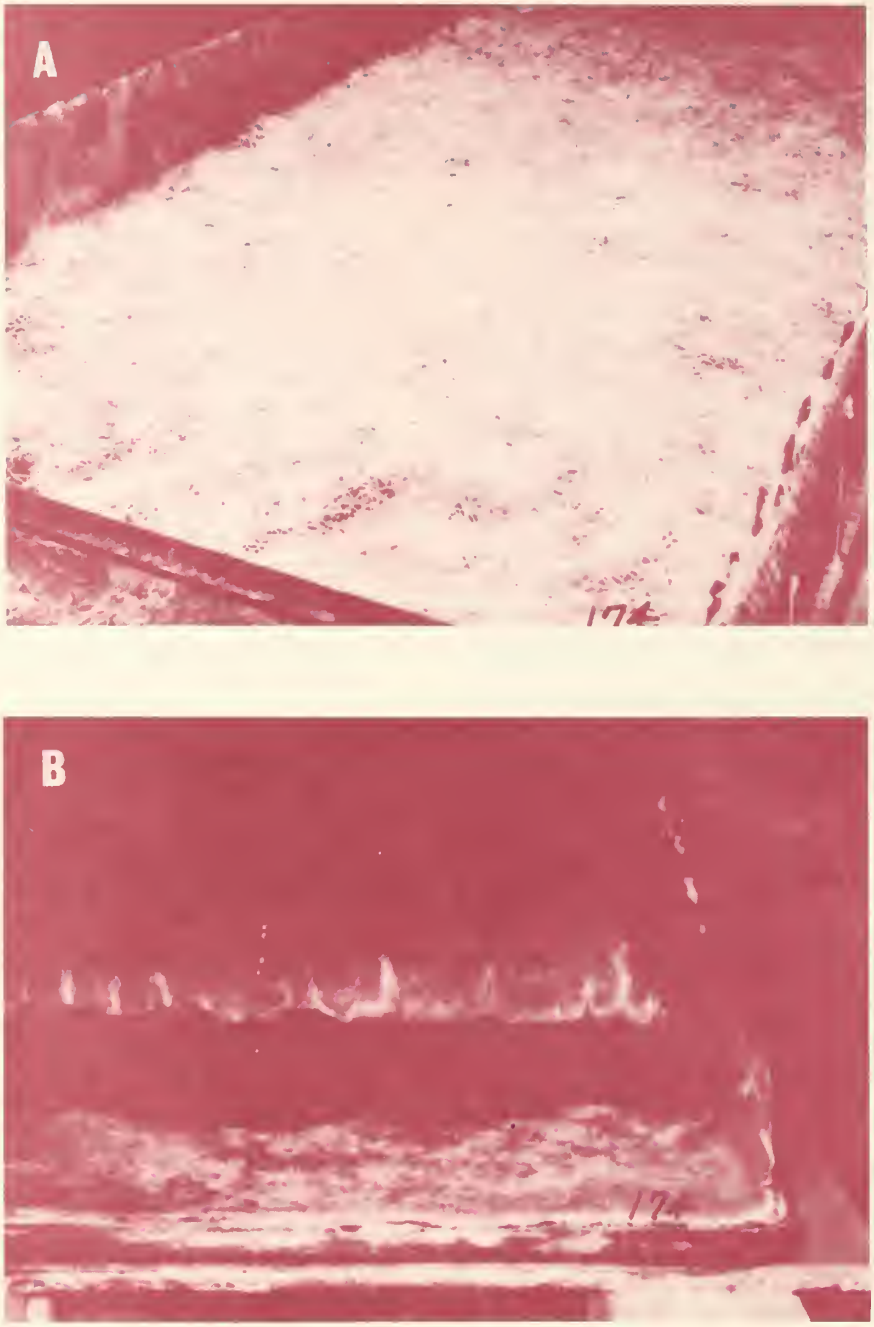

Figure 1.—Excelsior fuel bed for burn No. 174(A) and trailing edge view of the fire (B). σ = 81.3 cm^{-1}, β = 0.04, δ = 1.27 cm, w_o = 0.201 kg/m^2, M_f = 0.103, R = 0.269 m/min, and MBI = 0.6.

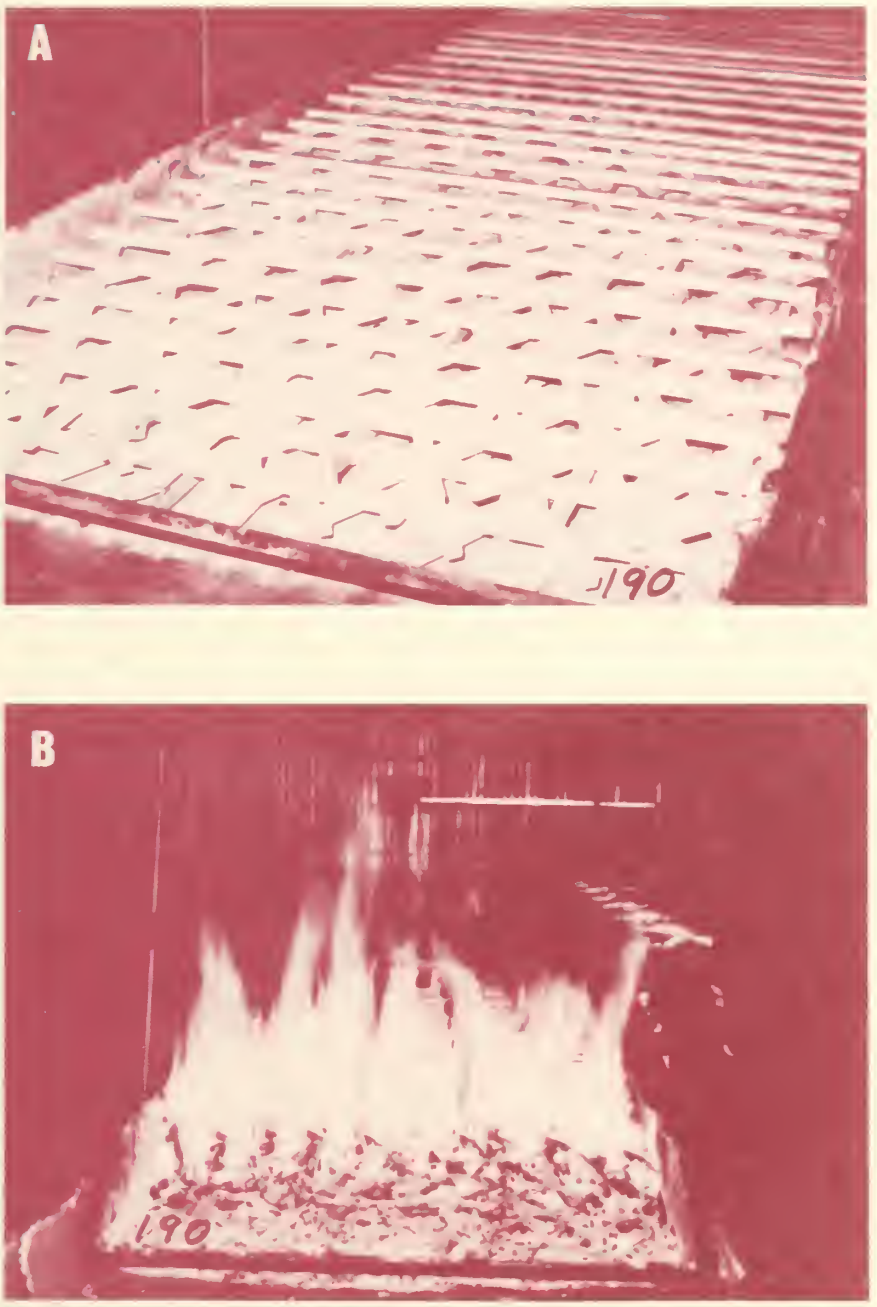

Figure 2.—Preburn 1/2-inch-square-stick fuel bed (A) and trailing edge view of fire (B). Burn No. 190. σ = 3.15 cm^{-1}, β = 0.16, δ = 10.16 cm, w_o = 7.16 kg/m^2, M_f = 0.165, R = 0.50 m/min, and MBI = 1.0.

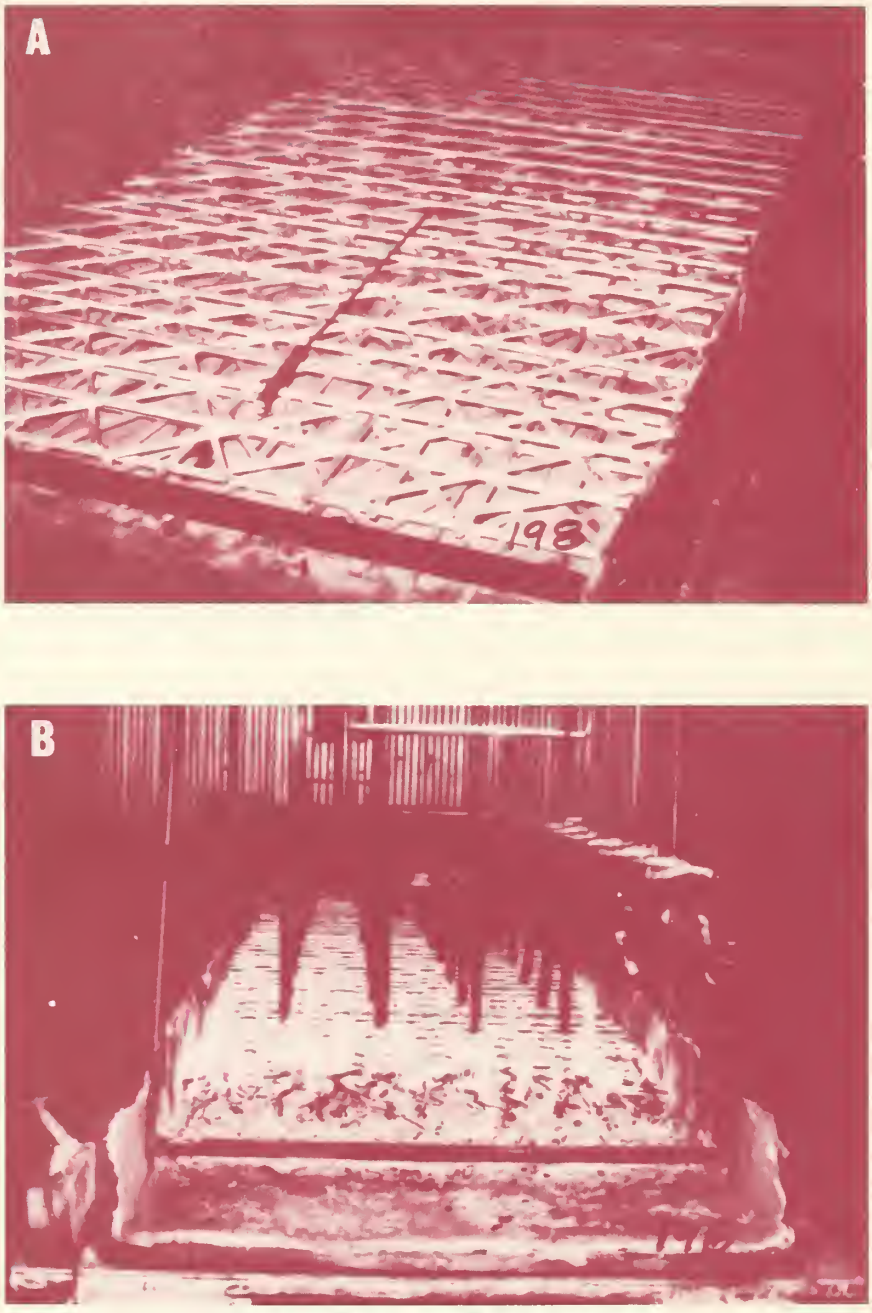

Figure 3.—Preburn 1/4-inch-square-stick fuel bed (A) and trailing edge view of fire (B). Burn No. 198. σ = 6.30 cm^{-1}, β = 0.08, δ = 5.08 cm, w_o = 1.790 kg/m^2, M_f = 0.181, R = 0.039 m/min, and MBI = 0.9.

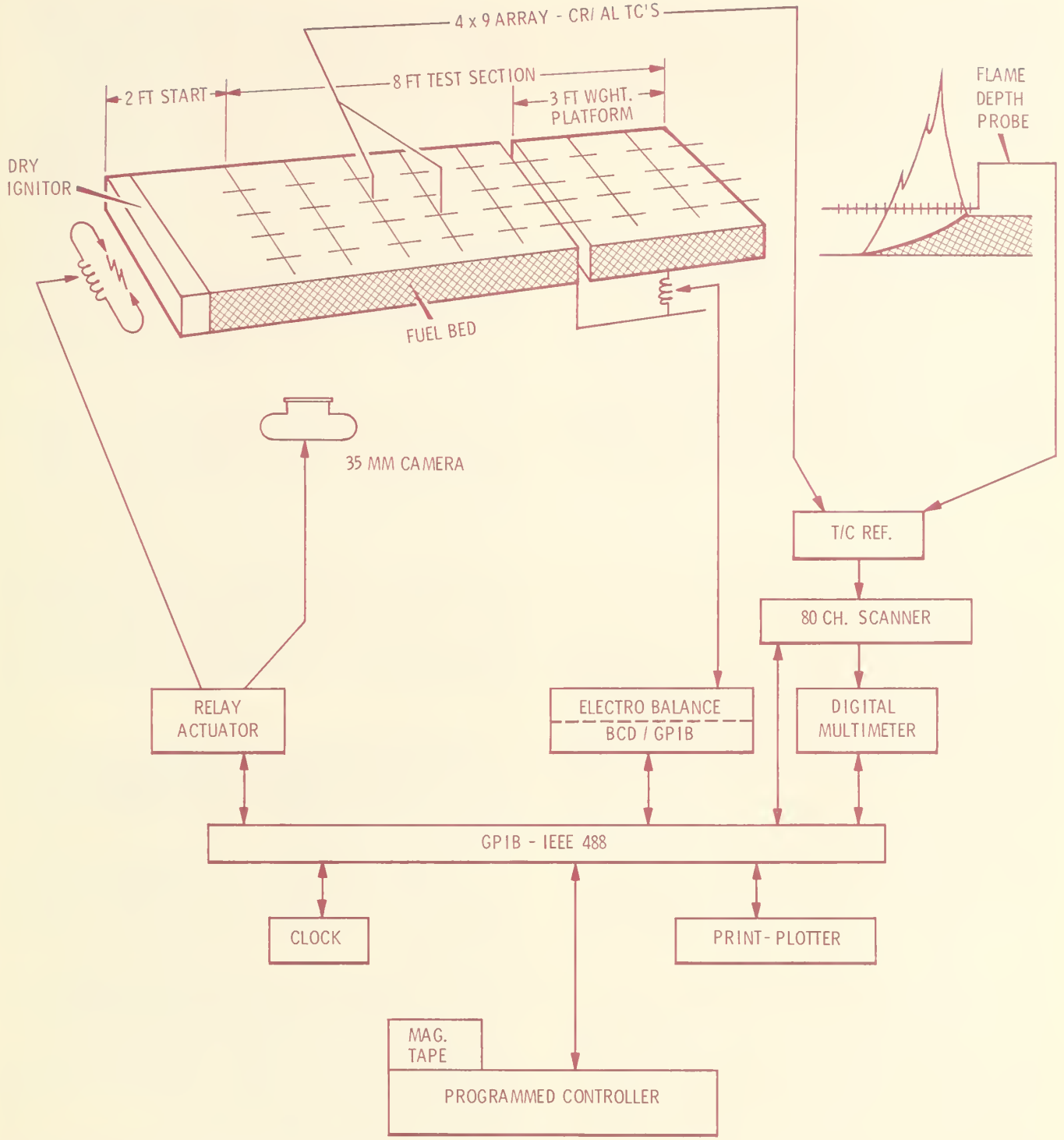

Figure 4.—Schematic of experimental instrumentation.

Immediately prior to ignition, fuel bed samples were bottled and sealed for later determination of fuel moisture by xylene distillation. Temperature and relative humidity in the combustion chamber were controlled at approximate conditions for the desired EMC during construction of the fuel bed and for the duration of the test fire.

Spread Rate

The measurement of spread rate was straightforward. A 9 row by 4 column (fig. 4) array of type K (Cr/Al) thermocouples was suspended 2 to 3 cm above the fuel bed surface on a spacing of 17.8 cm (7 in) between columns and 30.48 cm (1 ft) between rows. The TC's voltage was monitored at 1.5 to 2 s cyclic rate. When the thermal EMF exceeded 10 mv threshold (set to 5 mv for low-intensity fires) indicating arrival of the flame front, the clock time, T (i,j), was recorded for each thermocouple (identified by the jth row and ith column). The spread rate, R, was calculated by least squares fit to the equation

$$T = t_o + \left(\frac{1}{R}\right)X$$

where

T is elapsed time and X is distance burned (fig. 5).

Reaction Intensity

Reaction intensity is defined as $I_R = -h\,(dw/dt)$. The heat of combustion, h, was measured for each lot of fuel by oxygen bomb determination (table 2). The mass loss, dm/dt (fig. 6), was calculated from weight and time measurements recorded as the fires progressed over the last three feet of the fuel bed (fig. 4). The unit area weight loss rate, dw/dt, is the raw mass loss rate divided by the combustion zone area. The area of the combustion zone is determined by the width of the fuel bed and the flame depth discussed below. The weight loss rates (listed in column 13 of appendix table 5, are further corrected for fuel moisture by $1/(1 + M_f)$ where M_f is the fractional fuel moisture from the xylene distillation determinations.

Flame Depth/Residence Time

Rothermel (1972) defines reaction time, τ_R, as the "time taken for the fire front to travel a distance equivalent to the depth of one reaction zone." Reaction zone, here called flame depth (D_f), has never been precisely defined, much less the definition standardized.

It is left to the experimentalist to define this reaction/combustion/flame zone depth by his specific measurement technique.[3] Further difficulty is encountered in measuring the area of the combustion zone (by whatever methods including the present), because of its large inherent variance compared to other parameters.

Anderson (1964) and Rothermel and Anderson (1966) calculated the horizontal combustion zone depth, D_f, by measuring the residence time, t, that accrued while embedded thermocouples remained above a threshold temperature as the fire passed at a speed, R. Then $D_f = tR$. Rothermel (1972) measured a similar residence time from the weight loss curves as the combustion zone passed over the leading edge of the weighing platform.

In the tests reported here, the combustion zone depth is the horizontal distance from the leading to trailing edge of the base of the flame. Flame depth was measured by two direct methods; occasionally these results were checked with results using Rothermel's method when data and burning conditions were deemed appropriate (fig. 7A)—i.e., when no observable burnout existed and the burning fuel did not collapse onto nor bridge the weighing platform during transition of the combustion zone.

The primary experimental measurement of flame depth (listed in column 15 of appendix tables 5, 6) is the direct measurement (meter stick) of the distance from leading to trailing edge of the flames. Eight such measurements were taken manually and averaged for each fire (inset fig. 7B).

In addition, several flame probes were constructed of linear arrays of thermocouples for immersion in the flame 1 to 2 cm above the fuel bed (fig. 4). The thermocouple temperature profiles were measured coincident with the eight manual measurements of flame depth (fig. 7B). In the example shown (burn number 141), flame depth, D_f, is calculated:

$$D_f = (\Sigma \overline{\Delta T_i} \overline{\Delta X_i})/\overline{\Delta T}_{max}.$$

Flame depths measured in this manner are consistently 15 to 25 percent larger than the manual measurements and invariably smaller than those calculated by the weight loss technique.

The thermocouple probes were incapable of resolving flame depths, smaller than 5 to 6 cm (less than two intervals between thermocouples) or of measuring large zones when the flame depth approached the maximum length of the probe.

We subjectively observed, during the burning and analysis of these fires, that our experimental methods (Rothermel 1972; Anderson 1964; and present studies) may overestimate the combustion zone area that contributes to propagation of the leading edge of the fire. This is particularly likely to happen in heavy fuel loadings where the trailing edge burnout is not in a position to contribute heat flux to driving the fire.

These efforts to measure the total heat release of the combustion zone may provide (in most cases) adequate empirical relations for estimating flame lengths and other fire effects. But the empirical calculation of a gross "propagating flux ratio" masks the physical process by which the propagating heat flux drives the fire. It should be possible to define or experimentally determine a characteristic path length through (or flame depth into) the combustion zone beyond which little or no heat flux can reach the unburned fuel and by which fire propagation could be physically described, namely, by a balance of driving heat flux and preignition heating.

[3] The author fully appreciates the following view expressed by F. A. Albini (private communication 1981): "The problem here is that the idealization of the spreading fire as exhibiting two distinct event boundaries, one marking the onset of flaming combustion and one its termination, is not a wholly accurate one. We seek to preserve this idealization of the process for its power as a modeling concept, leaving the experimentalist the ill-defined task of fixing an operational definition of its measurement."

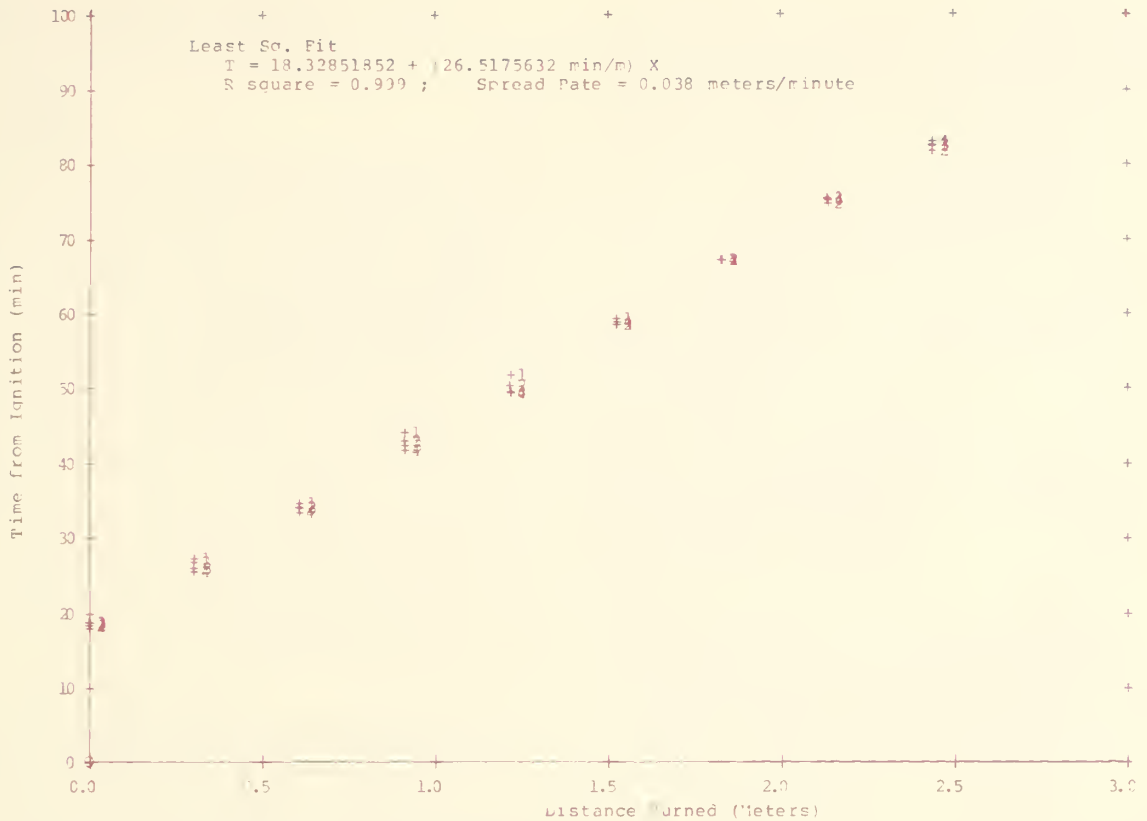
Least Sq. Fit
T = 18.32851852 + 26.5175632 min/m) X
R square = 0.999 ; Spread Rate = 0.038 meters/minute
Time from Ignition (min)
Distance Burned (Meters)

Figure 5.—Plotted data for rate of spread for burn No. 141.

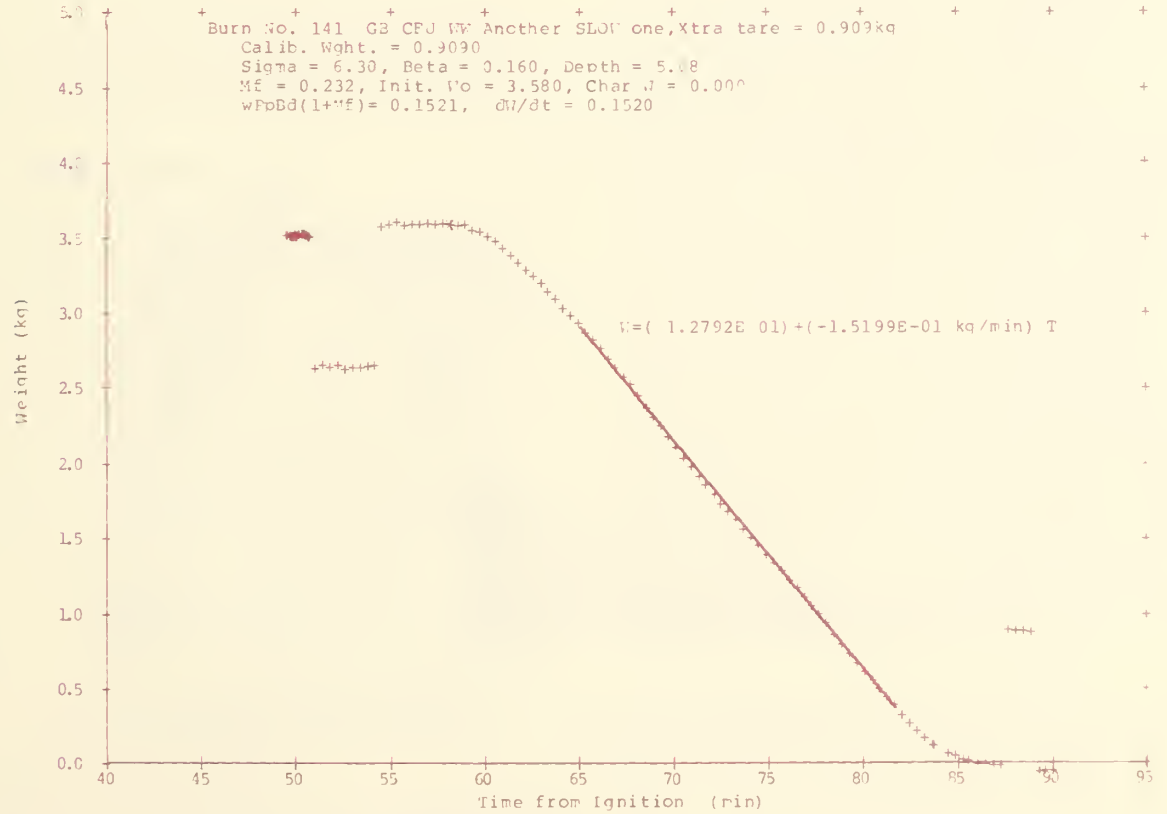

Figure 6.—Plotted data for mass loss rate for burn No. 141.

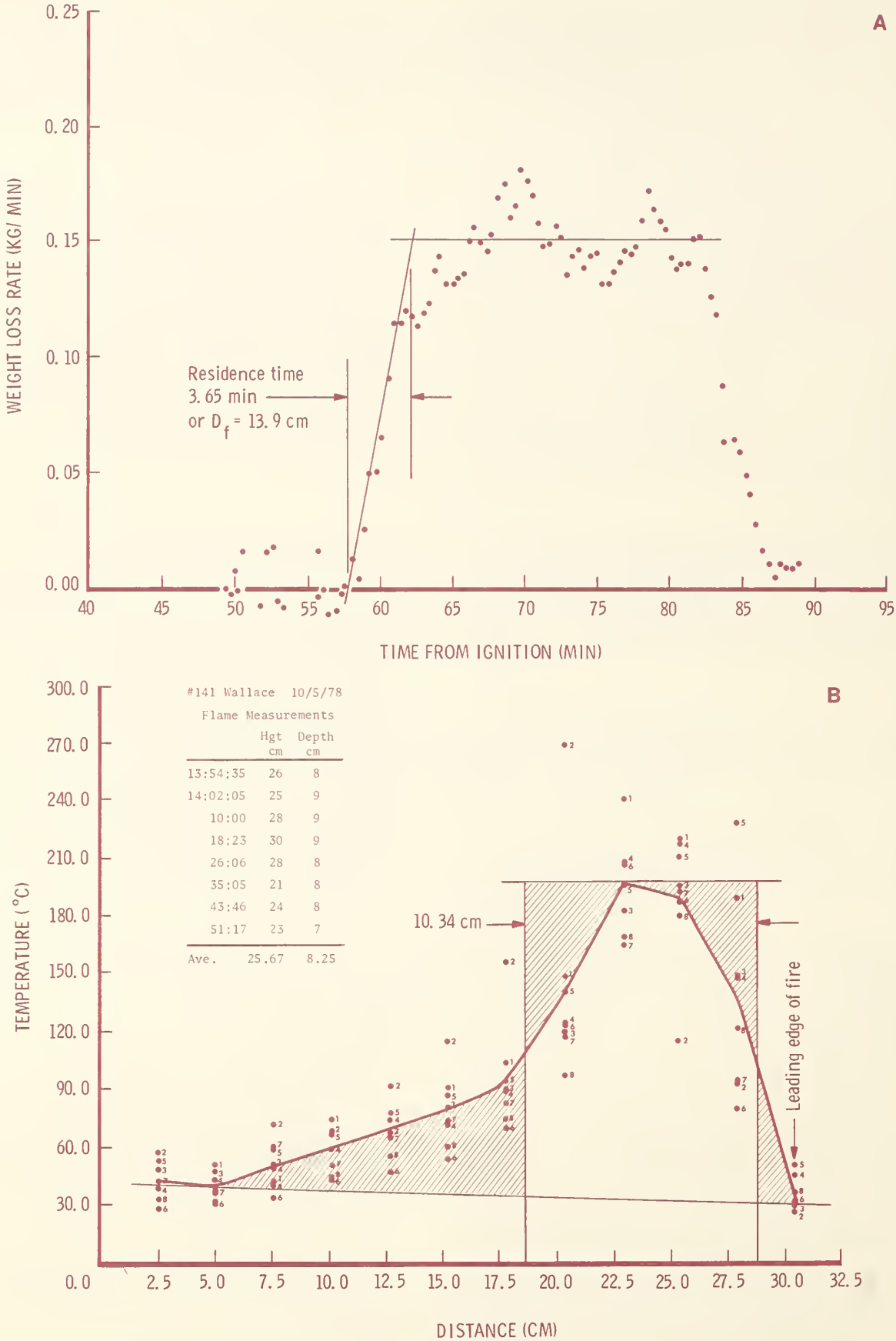

Figure 7.—Combustion zone depth from plotted weight loss rate (A) and from flame probe temperature profile (B) for burn No. 141.

This concept of an effective combustion zone depth might also be extended to eventually include the effects of wind on the fire.

Flame Height

Flame heights are not required in this analysis, but are recorded here to facilitate associated fire modeling studies. Visual/manual measurements of flame height (H_f) column 14, appendix tables 5 and 6, were made simultaneously with the flame depth measurements (8 observations for each fire). These are the observer's estimate of the spacial and temporal average flame height across the flame zone for several (5 to 10) seconds. The flame height measurement is particularly prone to observer bias. The individual "official" experimental observer making the H_f and D_f measurements was changed at burn number 61. In addition, periodically one or two (of six individuals) were asked to make simultaneous independent H_f and D_f measurements. A linear bias factor was calculated by least square regression routine with a dummy variable for each observer for each of the eight observers; the resulting H_f (and D_f) measurements listed in appendix tables 5 and 6 are normalized to the H_f (D_f) estimate of the average observer.

Another precautionary note concerns data taken of flames by photography—particularly by cameras with automatic exposure adjustments. It is obvious, but sometimes forgotten, that the dimensions of flames in photographs are very much dependent on the camera exposure settings. Longer exposures show higher peak flame tips and wider flame bases than do shorter exposures. Flame photographs were taken coincidently with the eight measurements of each fire, but were found to be unusable for numerical data on flame size. Nevertheless, the photos proved valuable for estimating the general state of combustion.

Index of Marginal Burning

It became evident during the study that the effect of fuel moisture on burning rate followed a regular pattern, dependent primarily on fuel size class and moisture content. The trend was monotone and regular except that the moisture content at which the fires became erratic or went out varied widely and unpredictably. Thus an arbitrary "Marginal Burning Index" (MBI) was constructed with values between -1 and 1 to indicate each fire's proximity to extinction. Fires that went out (self-extinguished) were given an MBI equal to the negative value of the fraction of unburned fuel bed length; a fire that burned out 1 ft into the 10-ft-long conditioned fuel bed was given MBI $= -0.9$, one that burned out at 4 ft had MBI $= -0.6$, and so on. Secondly, the self-sustaining fires were given an MBI value equal to the fraction of bed width, with flame based attached to the combustion zone as measured on the end view photos (fig. 1). These MBI values are in column 16 of appendix tables 5 and 6.

DISCUSSION OF RESULTS

The study plan was designed so that we could partition the data and examine each independent variable, holding all others constant. Because additional data are to be collected, only a gross overview of preliminary results is presented here.

The statistical bias possibly introduced by the log transforms was examined briefly, found negligible, and then ignored; that is, for

$$y = I_R, \Gamma', \xi, \eta_M, \text{ etc.}$$

under some conditions the expectation value,

$$\langle y \rangle = \exp(\langle \ln y \rangle + S^2_{\ln y}/2)$$

where from the linear regression (eqn. 6, 9, 12)

$$\langle \ln y \rangle = \Sigma C_i X_i$$

and $S^2_{\ln y}$ is the variance of ln y.

In the following discussion the expectation values $\langle y \rangle$ (or predictions, $\hat{y}$) are estimated by neglecting the transform bias, thus

$$\langle y \rangle = \exp(\langle \ln y \rangle).$$

Reaction Intensity, Reaction Velocity

The self-sustaining fires were partitioned by fuel size class, σ, then multiple linear regressions performed on the log transformed form of equation 6 (equation 12).

$$\ln(I_R) = C_1 + C_2 \ln(\beta) + C_3\beta + C_4 \ln(\delta) + C_5 M_f. \quad (12)$$

The regression coefficients are listed in table 4; for comparison, the equivalent coefficients of Rothermel's (1972) formulas are also listed. The standard error associated with each coefficient is included in parentheses, and the standard error and r^2 of each regression is also listed.

The apparently constant value of C_1 for all three sizes of fuel needs further confirmation and analysis. From Rothermel's limited data, values for this parameter increased with increasing fuel particle size (smaller surface/volume, σ). On cursory examination of equation 5 (taking liberty against formal rigor), as the packing ratio nears its optimum value, $(1 - C_2)/C_3$, the reaction intensity, $I_R = (w_o/\rho_p)e^{C_1}$. The new results imply that the reaction intensity per unit mass of dry fuel at the optimum packing may be a constant,[4] independent of fuel size or that a free-burning fire may be correctly modeled by a burning rate (mass loss) that is proportional to the total fuel surface area (per unit area of bed)—thus providing a mechanism for handling fuel beds of mixed fuel sizes (note also that if the above proves true, then β_{op} may be determined from **stationary** crib fires with much better experimental accuracy). This sketchy speculation will be examined and studied further with test fires of fuels in the intermediate sizes, $10 < \sigma < 50$ cm^{-1}.

[4]This result is similar to that cited by Harmanthy (1972) where room and compartment fires with essentially unrestricted ventilation had nearly constant (0.0062 kg/m^{2}s) burning (massloss) rates per unit area of fuel surface. Our present equivalent value (from C_1 above) of approximately 0.003 kg/m^{2}s is within the lower range of values from Harmanthy's sources. Thomas (1960) found similar values (0.0021 to 0.0062 kg m^{2}s) for 1-cm-square sticks in stationary crib fires.

The C_4 coefficient is very close to unity for the two larger fuel sizes and reinforces Rothermel's assumption that the reaction intensity is linear with fuel loading. In the fine fuel (excelsior, $\sigma = 81.3\ cm^{-1}$) the fractional value of C_4 (0.65) indicates a weaker dependence (of I_R on loading) at these loadings and packing ratios. The study was designed to have similar loadings and packing ratios for all fuel sizes within the physical limits of packing the fine fuels. In many of the fires in fine fuels the trailing edge of the combustion zone was not in position to contribute to driving the leading edge of the fire particularly in the deeper, heavier fuel beds—having the effect of decreasing the dependence of reaction intensity on loading.

We plan to extend the fine fuel data base to lighter loadings in the near future. This extension will include loadings near 20 gm per square meter and packing ratios of 0.0005, which approach the light loading limits found in forest litter and grass fields.

In figure 8 A, B, and C, the reaction intensity curves and data (corrected to $M_f = 0$) are plotted and compared with those of Rothermel (1972). For ease of comparison the weighted averages of data at each packing ratio are shown.

In figure 9 A, B, and C, the reaction velocity is similarly compared. The above remarks concerning the fine excelsior fuels are again apparent; in addition, we note that Rothermel forced the reaction velocity curve (for the fine fuels) through the origin by heuristic argument to obtain a maximum Γ' and β_{op}. Figure 9 B and C, show significant differences in the old and new maxima of the reaction velocity curves for the larger fuel sizes. These are the maxima that determine the optimum packing ratios, β_{op}. A review of both the old and new raw data indicates that Rothermel's mass loss rates tend to level off with heavier loading (larger β) and, more importantly, his residence time (or flame depth) increased significantly with larger packing ratios (see discussion of flame depth measurements above).

Lacking data for light loading in the fine fuels, it is premature to draw new conclusions. Also, data are needed in the intermediate size fuels ($10 < \sigma < 50\ cm^{-1}$) before definitive improvements are made in the present fire equations.

Propagating Flux Ratio

The regression coefficients, d_i, for the propagating flux ratio, ξ, (equation 9), are included in table 4. The regression curves, data, and Rothermel's original curves are compared in figure 10 A, B, and C. Although the coefficients in the empirical regression equations differ considerably, the original Rothermel curves are still reasonable approximations—with the possible exception of underestimating the propagation intensity in the fine fuels.

The data shown in figure 10 suggest that a linear form of ξ (rather than the exponential) may be a better approximation. The best least squares fit of several alternative forms (each including all experimental fires) is

$$\xi = 0.017 - 0.317\,\beta + 0.1119\,(\sigma\beta)$$

with $r^2 = 0.91$, standard error $= 0.048$; the standard error associated with the coefficient (0.1119) of the product $(\sigma\beta)$ is 0.0026.

The product $(\sigma\beta)$ has the physical interpretation of a radiation extinction coefficient for the fuel bed. Its significance as a parameter in the propagation intensity is supported here. Tests of this relationship will be extended by experimental data in the intermediate size fuels ($10 < \sigma < 50\ cm^{-1}$).

Fuel Moisture

We may interpret $(-1/C_5)$ as a characteristic fuel moisture, M_σ, dependent on fuel particle size (surface/volume ratio):

$$\eta_M = \exp(C_5 M_f) = \exp(-M_f/M_\sigma).$$

The characteristic moisture M_σ is, then, the fuel moisture at which the reaction intensity falls to 1/e of its value at $M_f = 0$. It can be argued heuristically that M_σ must approach a constant value in the fine fuel limit (σ large) and that M_σ should have a small positive value for very large fuels (σ small) and that it must fit the $1/C_5$ values in table 4; then

$$M_\sigma = 1/(2 + 2.4 \exp(-0.179\sigma))$$

empirically described the relation of M_σ to fuel particle size, σ, for σ expressed in cm^{-1}. Observe parenthetically that the factor 0.179 (cm) in the equation above is a characteristic "fuel particle surface depth" associated with fuel moisture and fire propagation, and that it is comparable to Frandsen's (1973) depth coefficient (1/138 ft = 0.22 cm) in his effective heating equation.

The function M_σ is plotted in figure 11. This curve again demonstrates the need for confirming experimental data for fuels in the range of $10 < \sigma < 50\ cm^{-1}$ (fuel particles of 1/8-, 1/16-, and 1/32-inch thickness) near the knee of the M_σ curve.

Figure 12 is a plot of the moisture-damping curve with the confidence bands for each of the three fuel particle sizes. The bands are calculated from the standard error of the coefficient C_5 alone and are given here at the 67 percent confidence level, which is ± one standard error (Draper and Smith 1966).

The curve fit (fig. 12) includes all fires (however broken up, erratic, or marginal) that did not go out.

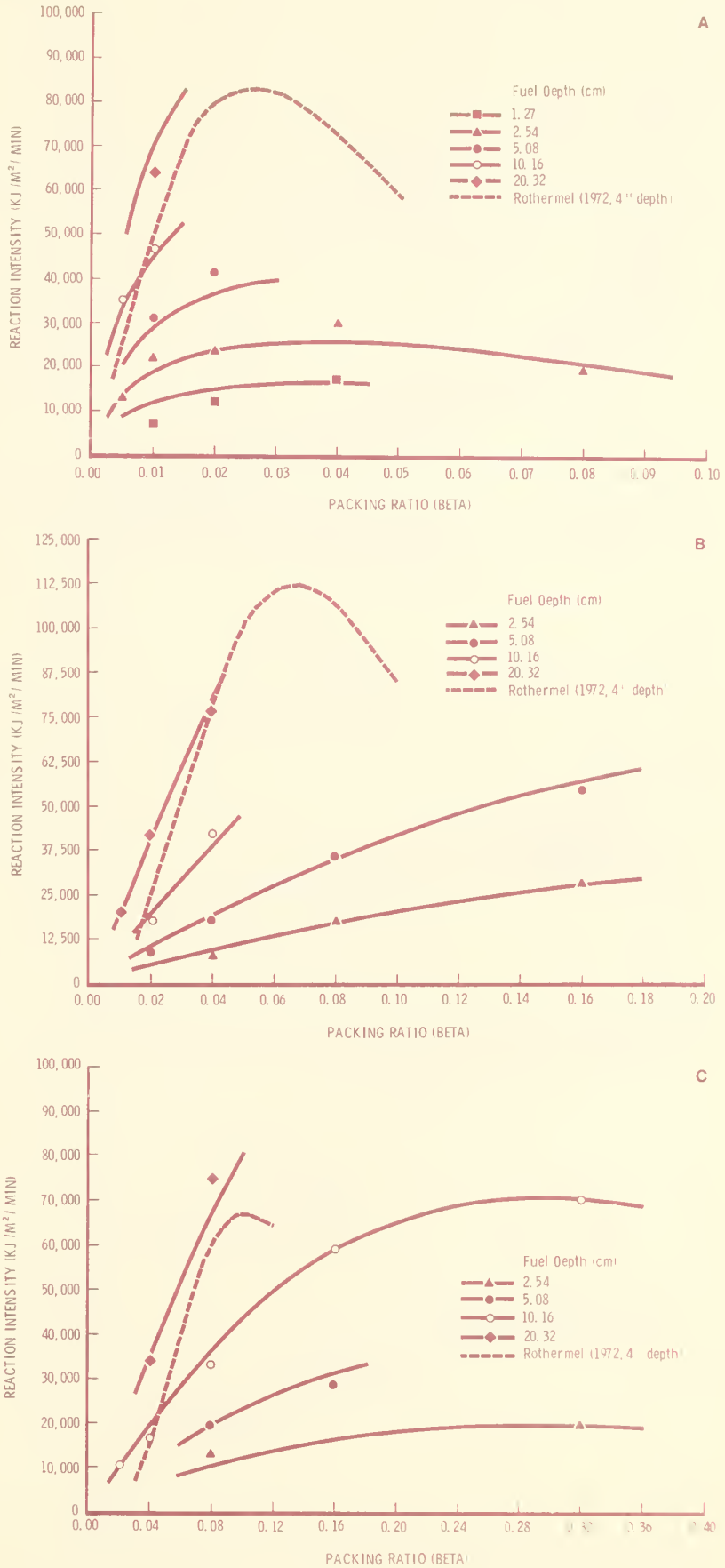

Figure 8.—Reaction intensities for excelsior (A), 1/4-inch fuels (B), 1/2-inch fuels (C).

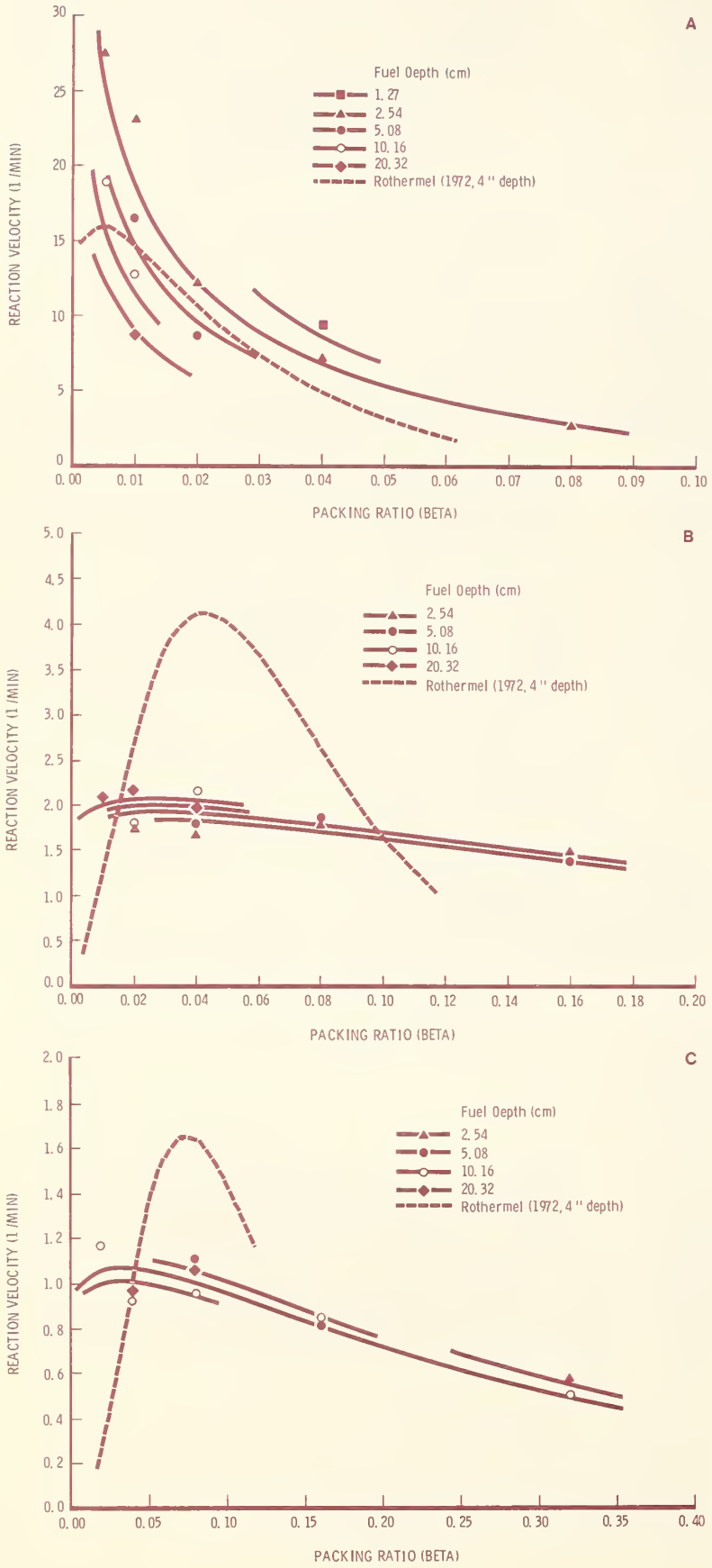

Figure 9.—Reaction velocities for excelsior (A), 1/4-inch fuels (B), 1/2-inch fuels (C).

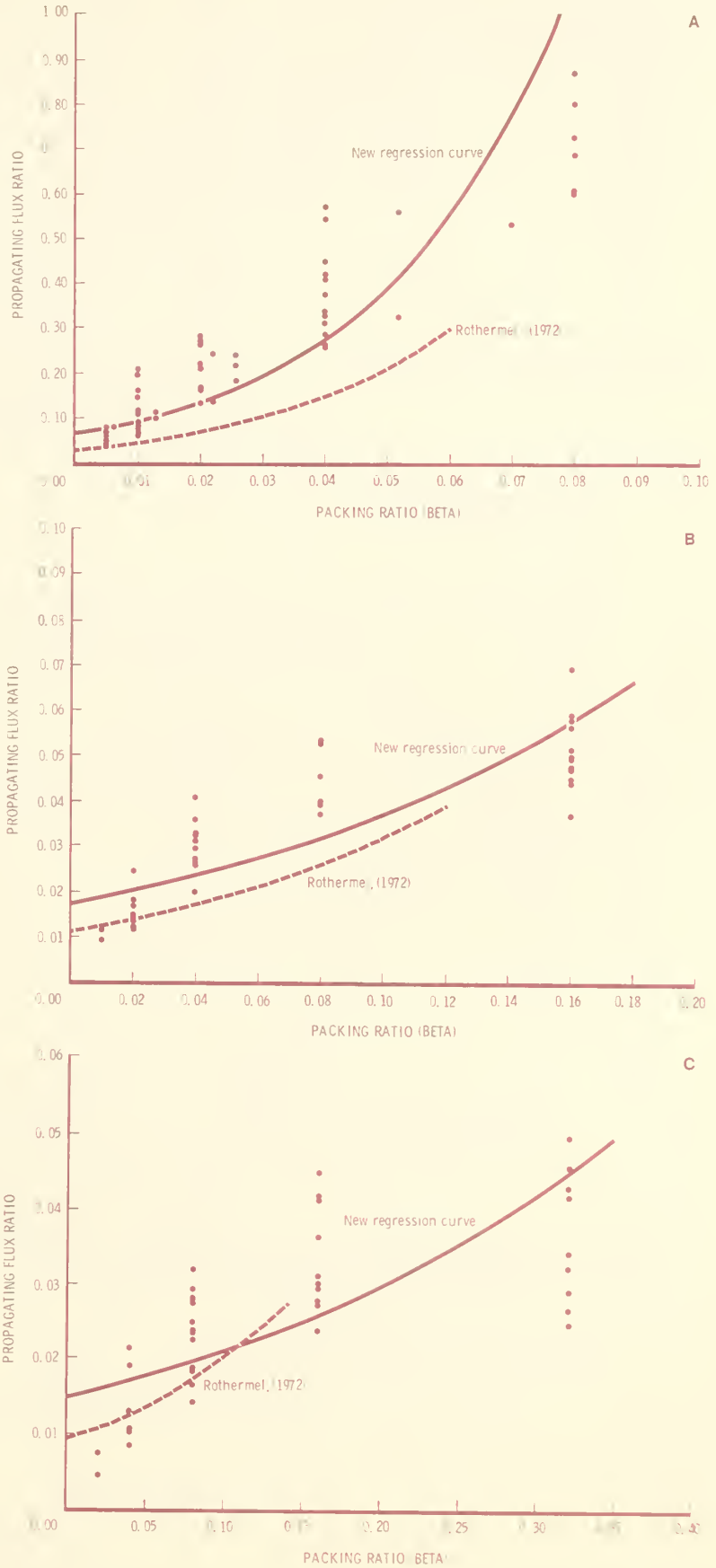

Figure 10.—Propagating flux ratio for excelsior (A), 1/4-inch fuels (B), 1/2-inch fuels (C).

Table 4.—Regression coefficients

Coefficients	σ = 81.3 cm^{-1}			σ = 6.3 cm^{-1}			σ = 3.15 cm^{-1}		
	New value	Standard error	Old value[1]	New value	Standard error	Old value[1]	New value	Standard error	Old value[1]
C_1	11.985		14.95	11.81		20.70	11.542		23.91
C_2	.574	(0.088)	1.27	1.104	(0.076)	3.075	1.143	(0.090)	4.591
C_3	-14.85	(3.32)	-49.29	-3.432	(1.03)	-45.93	-3.828	(.66)	-45.06
C_4	.652	(.035)	1.000	1.053	(.038)	1.000	.923	(.048)	1.000
C_5	-1.969	(.17)		-2.735	(.250)		-3.570	(.335)	
r^2	.82			.95			.92		
SE	.25			.128			.156		
β_{op}	(—)		.0056	.030		.045	.037		.080
d_1	-2.633		-3.258	-4.032		-4.465	-4.183		-4.633
d_2	34.07	(2.02)	34.69	7.336	(.819)	10.23	3.413	(.644)	7.465
r^2	.75			.62			.39		

[1] Equivalent value calculated from Rothermel (1972).

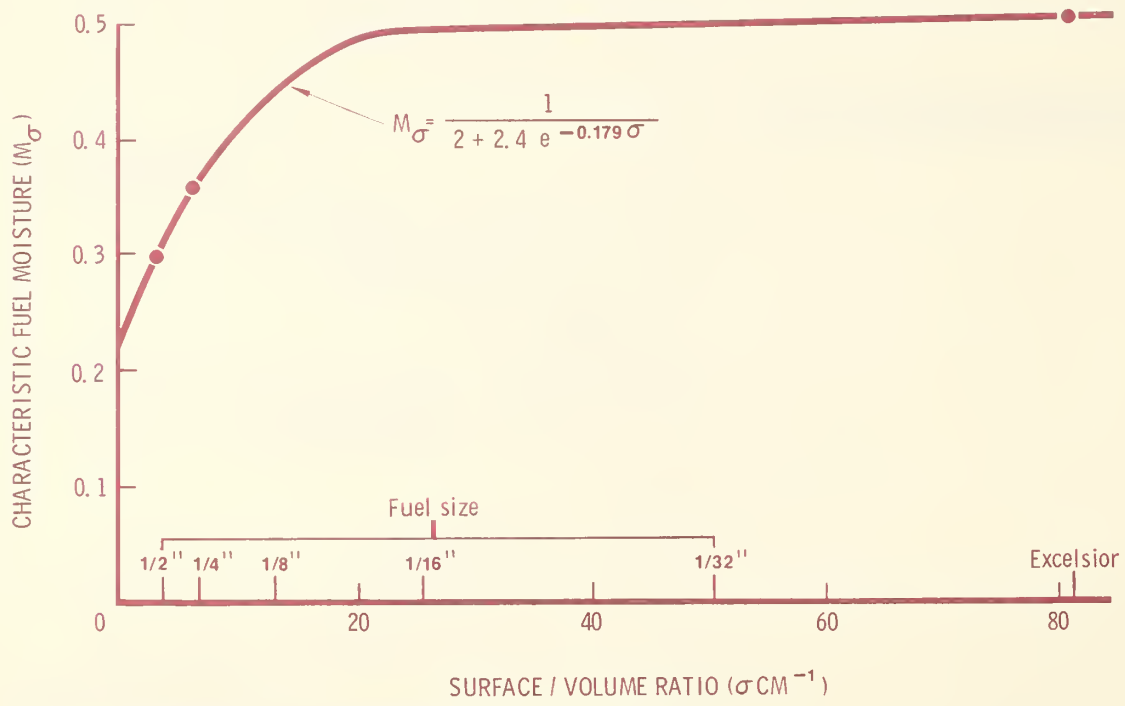

Figure 11.—Fuel moisture characteristic of fuel particle size.

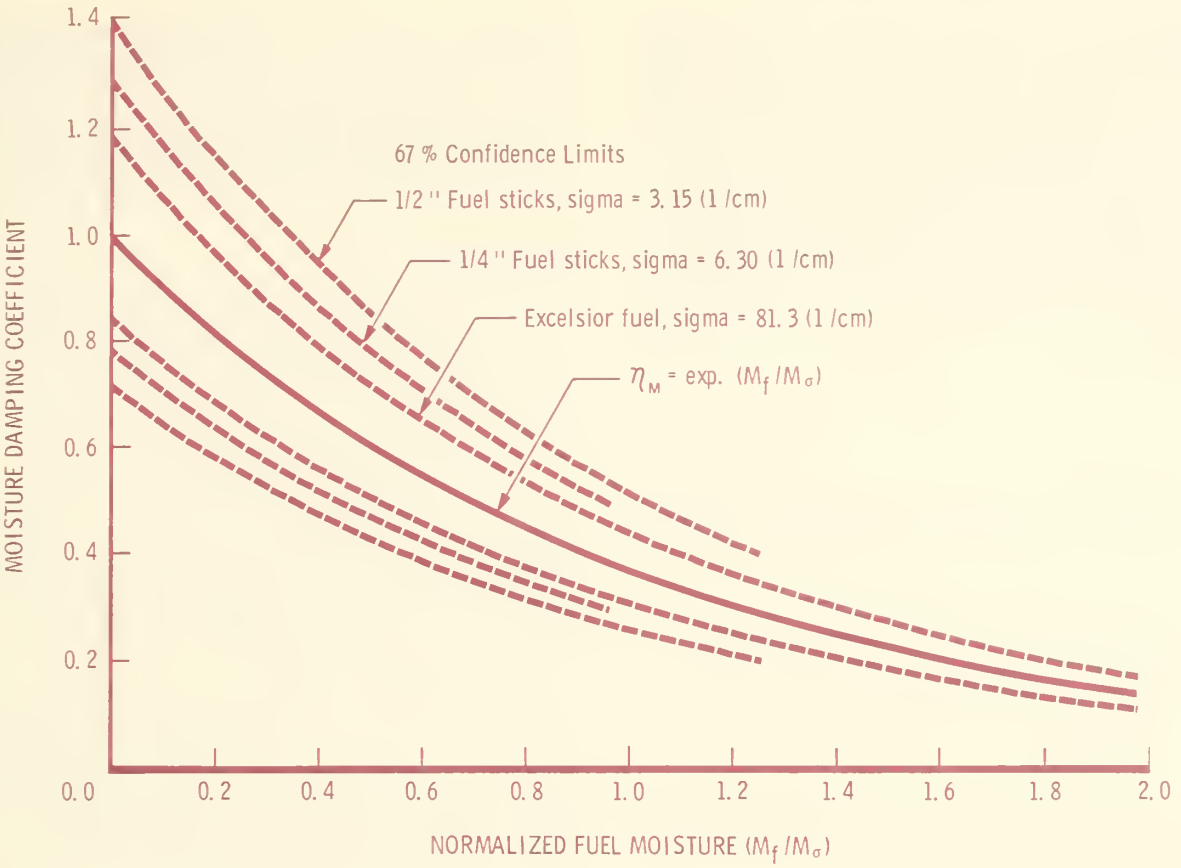

Figure 12.—Moisture-damping coefficient, with expected error at 67 percent confidence level (± one standard error on the coefficient, C_5).

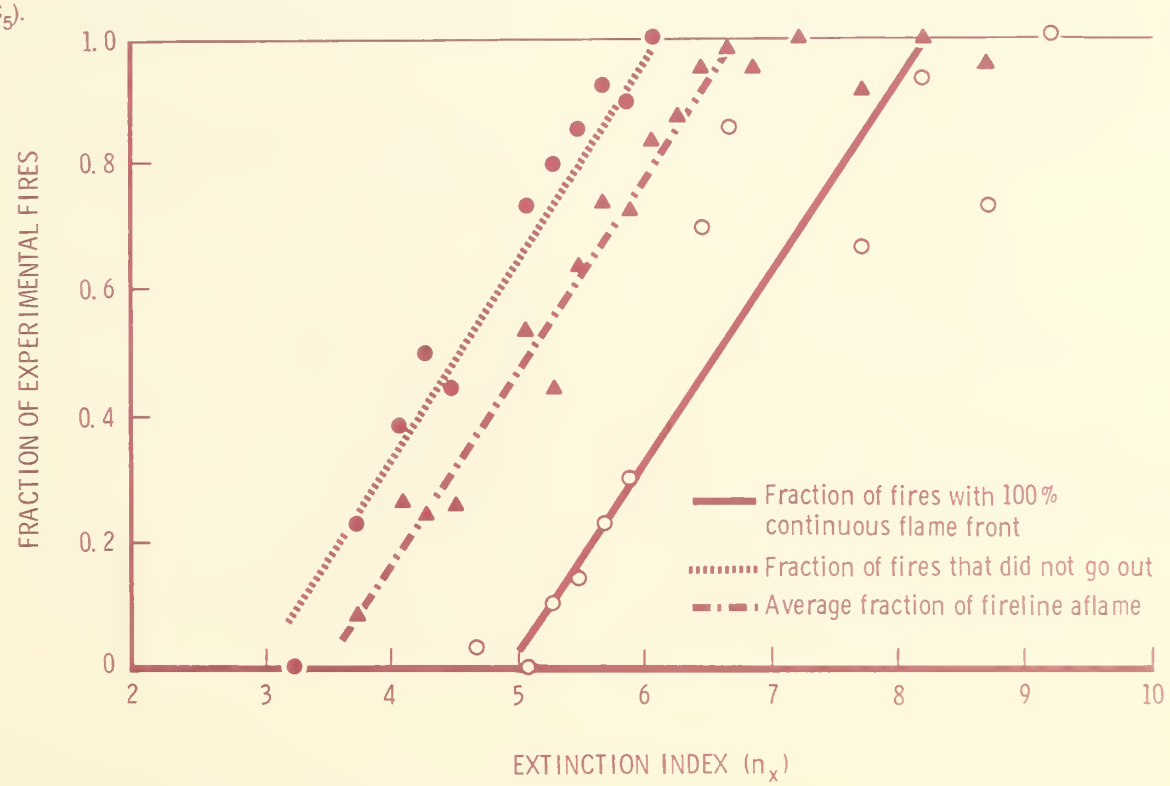

Figure 13.—Probable fire states near extinction.

Extinction

As indicated above, the product $\sigma\beta\delta$ is the total fuel particle surface area per unit area of fuel bed. One might expect, as surface area of fuel decreases, that fires will be more difficult to burn and, conversely, as the fuel surface area becomes large, fires will burn more easily and burn at higher fuel moisture. Indeed, as the experimental burning progressed, a predictive rule-of-thumb was developed—fires will not burn if the fuel moisture exceeds:

$$M_f \geq (\ln (2\ \sigma\beta\delta))/4,$$

or if

$$\sigma\beta\delta \leq \exp (4M_f)/2.$$

From this subjective observation and iterative review of the experimental data, a family of curves,

$$\sigma\beta\delta = 2^{(k/2-3)}\exp(-kM_f) \quad \text{for } 0 < k < 20$$

was developed that partition the experimental fires at relatively constant MBI (see Marginal Burning Index above). Thus, an extinction index, n_X, is defined:

$$n_X = \frac{\ln (8\ \sigma\beta\delta)}{M_f + \ln \sqrt{2}} \qquad (15)$$

as a predictive indicator of marginal burning. Large values of n_X indicate greater likelihood of good burning; small values, poorer burning. The experimental data, MBI, is compared with n_X in figure 13. The index, n_X, was calculated for each fire; values ranged from 2.56 to 13.56. The number of fires was counted within successive increments of n_X, and classified (1) as a "no burn" with zero flame; (2) by the fraction of flaming fire front (described above), or (3) as a "steady state" fire with 100 percent continuous flame front. The average fraction of flaming front was calculated (for the class 2 fires) within each increment of n_X. Thus, the left most curve of figure 13 represents a probability, P_o, that fires may burn (not go out).

$$P_o = -0.885 + 0.3077\ n_X, \quad (2.875 \leq n_X \leq 6.125). \qquad (16)$$

The central curve,

$$P_m = -1.077 + 0.3077\ n_X, \quad (3.5 \leq n_X \leq 6.75), \qquad (17)$$

represents the average fraction of fireline aflame; and the right-hand curve,

$$P_{ss} = -1.538 + 0.3077\ n_X, \quad (5 \leq n_X \leq 8.25), \qquad (18)$$

is the probability of steady state burning (full, continuous flame front). Fuels will not burn if $n_X < 2.87$; if $n_X > 8.25$, then fires will burn well with a hot, continuous flame front.

Analysis of extinction lacks the rigor that will come later along with more definitive data; however, two points are illustrated; first, that the conditions of marginal burning are experimentally managable and not completely unpredictable (ref. the M_X rationale problem); second, the fuel moisture-surface area relationship provides a mechanism whereby the marginal limits of burning are conditional on fuel loading and particle size as well as fuel moisture content.

SUMMARY

The original assumption that the reaction intensity in the combustion zone is linear with loading is experimentally supported within the fuel sizes, loadings, and packing ratios commonly encountered in wildland fuels; further confirmation is needed in light loadings of the fine fuels.

Rothermel's empirical relations for the propagating flux ratio are judged adequate for current use, though perhaps they underestimate the propagating flux in heavy loads of fine fuels. New evidence is found to physically relate the propagating flux ratio to the optical density ($\sigma\beta$) of the fuel bed. Again, further development is needed.

Experimental difficulties in rigorous determination of reaction zone size remain unsolved. Thus, physical interpretation of reaction intensities should be made with caution. Similarly, the causes and consequences of the optimum packing ratio should be interpreted with caution; for example (in the author's opinion) the widely held idea that reaction intensity is limited by oxygen supply (indraft) at heavier packing ratios is premature and has been overemphasized.

Confirmation is also needed for the hypothesis formed above that the heat release rate (reaction intensity) per unit of mass loading is constant—independent of fuel size. Heretofore, very little experimental evidence was available concerning the relative weighting factors for the several size classes found in wildland fuels. If confirmed, the rationale is that in free-burning fires, the burning mass loss rate will be proportional to the total fuel surface area per unit area of fuel bed.

The marginal limit of self-sustained burning is a function of the fuel surface area as well as fuel moisture content. Thus, an independent function is proposed (for further investigation) as a predictive indicator of marginal burning. The form of the moisture-damping coefficient is much simplified by thus removing the requirement that it provide for the fire extinction limit. After removal of the extinction requirement from the fuel moisture-damping coefficient, it is apparent that the functional relation between moisture damping and fuel particle size becomes tractable.

Additional experimental data are needed in the intermediate fuel sizes and in the light loading limits of fine fuels before definitive conclusions can be made.

An extension of the study in the light and intermediate fuels is underway.

PUBLICATIONS CITED

Albini, F. A.
1976. Computer-based models of wildland fire behavior: a user's manual. USDA For. Serv., unnumbered publ., 68 p. Intermt. For. and Range Exp. Stn., Ogden, Utah.

Anderson, H. E.
1964. Mechanisms of fire spread. Research Progress Rep. No. 1. USDA For. Serv. INT-8, 20 p. Intermt. For. and Range Exp. Stn., Ogden, Utah.

Draper, N. R., and H. Smith.
1966. Applied regression analysis. John Wiley and Sons, Inc., New York.

Frandsen, W. H.
1971. Fire spread through porous fuels from the conservation of energy. Combustion and Flame 16:9-16.

Frandsen, W. H.
1973. Effective heating of fuel ahead of spreading fire. USDA For. Serv. Res. Pap. INT-140, 16 p. Intermt. For. and Range Exp. Stn., Ogden, Utah.

Harmanthy, T. Z.
1972. A new look at compartment fires, part I. Fire Technology 8(3):196-217.

Rothermel, R. C.
1972. A mathematical model for predicting fire spread in wildland fuels. USDA For. Serv. Res. Pap. INT-115, 40 p. Intermt. For. and Range Exp. Stn., Ogden, Utah.

Rothermel, R. C., and H. E. Anderson.
1966. Fire spread characteristics determined in the laboratory. USDA For. Serv. Res. Pap. INT-30, 34 p. Intermt. For. and Range Exp. Stn., Ogden, Utah.

Thomas, P. H.
1960. On the rate of burning of wood. F.R. Note No. 446, 11 p. Fire Res. Stn., Boreham Wood, Hertsfordshire, England.

Wilson, R. E.
1980. Reformulation of forest fire spread equations in SI units. USDA For. Serv. Res. Note INT-292, 5 p. Intermt. For. and Range Exp. Stn., Ogden, Utah.

APPENDIX - TABULATED EXPERIMENTAL DATA

In the following data tables the columns in left-to-right order are: 1, tape file number; 2, chronologic order of fire; 3, group number; 4, 5, 6, ambient conditions of test chamber; 7, fuel moisture; 8, surface/volume ratio of fuel particles; 9, packing ratio (solid/total volume); 10, fuel bed depth; 11, initial ovendry loading; 12, fire spread rate; 13, dry mass loss rate (3-ft-wide bed); 14, average flame height; 15, average flame depth; 16, index of flame continuity.

Table 5.-- Experemental fire data.

File #	Burn #	Grp #	Temp C*	RH %	EMC (frac)	Mf (frac)	Sigma (1/cm)	Beta	Depth (cm)	Load (kg)	R (m/min)	dw/dt (kg/min)	FH (cm)	FD (cm)	FI
1	48	1	27.2	9	0.021	0.018	81.27	0.005	2.54	0.050	0.453	0.020	7.55	4.04	0.50
2	66	1	27.2	25	0.053	0.053	81.27	0.005	2.54	0.050	0.353	0.017	4.96	3.50	0.40
3	7	1	21.1	40	0.077	0.102	81.27	0.006	2.54	0.065	0.375	0.022	14.06	3.84	0.50
4	153	1	27.2	80	0.157	0.142	81.27	0.005	2.54	0.050	0.298	0.012	5.29	2.14	0.30
5	98	1	27.2	90	0.202	0.202	81.27	0.005	2.54	0.050	0.169	0.008	1.50	1.50	0.30
6	133	1	27.2	90	0.202	0.251	81.27	0.005	2.54	0.050	0.237	0.011	3.29	2.29	0.50
7	41	2	29.4	11	0.023	0.024	81.27	0.005	10.16	0.201	0.935	0.172	45.69	9.61	1.00
8	52	2	30.0	11	0.023	0.027	81.27	0.005	10.16	0.201	0.966	0.156	45.69	10.58	1.00
9	58	2	27.2	25	0.053	0.058	81.27	0.005	10.16	0.201	0.867	0.154	47.27	10.55	1.00
10	171	2	27.2	65	0.117	0.095	81.27	0.005	10.16	0.201	0.699	0.130	54.24	10.07	1.00
11	154	2	27.2	80	0.157	0.147	81.27	0.005	10.16	0.201	0.618	0.123	33.57	8.29	1.00
12	103	2	27.2	90	0.202	0.211	81.27	0.005	10.16	0.201	0.564	0.112	21.00	7.63	0.90
13	132	2	27.2	90	0.202	0.268	81.27	0.005	10.16	0.201	0.560	0.092	20.86	8.86	1.00
14	39	3	31.7	11	0.024	0.028	81.27	0.010	1.27	0.050	0.388	0.018	5.72	4.95	0.70
15	60	3	27.2	25	0.053	0.053	81.27	0.010	1.27	0.050	0.372	0.017	8.73	5.79	0.90
16	175	3	27.2	65	0.117	0.109	81.27	0.010	1.27	0.050	0.000	0.000	0.00	0.00	-0.70
17	152	3	27.2	80	0.157	0.139	81.27	0.010	1.27	0.050	0.279	0.013	4.29	4.29	0.40
18	97	3	27.2	90	0.202	0.203	81.27	0.010	1.27	0.050	0.000	0.000	0.00	0.00	-0.90
19	49	4	27.2	9	0.021	0.019	81.27	0.010	2.54	0.101	0.681	0.063	19.91	7.49	1.00
20	38	4	31.7	11	0.024	0.026	81.27	0.010	2.54	0.101	0.660	0.060	26.54	6.38	1.00
21	67	4	27.2	25	0.053	0.055	81.27	0.010	2.54	0.101	0.508	0.046	31.84	4.88	0.95
22	8	4	21.1	40	0.077	0.101	81.27	0.013	2.54	0.130	0.499	0.059	15.33	5.35	0.90
23	146	4	27.2	80	0.157	0.128	81.27	0.010	2.54	0.101	0.477	0.044	20.43	4.86	0.90
24	95	4	27.2	90	0.202	0.209	81.27	0.010	2.54	0.101	0.380	0.035	10.40	4.20	0.70
25	124	4	27.2	90	0.202	0.299	81.27	0.010	2.54	0.101	0.208	0.019	6.50	2.50	0.30
26	37	5	31.7	11	0.024	0.025	81.27	0.010	5.08	0.201	0.790	0.141	45.94	13.02	1.00
27	50	5	29.4	11	0.023	0.025	81.27	0.010	5.08	0.201	0.824	0.137	47.35	9.77	1.00
28	40	5	29.4	11	0.023	0.027	81.27	0.010	5.08	0.201	0.802	0.130	46.45	8.63	1.00
29	65	5	27.2	25	0.053	0.056	81.27	0.010	5.08	0.201	0.554	0.099	34.92	7.29	1.00
30	59	5	27.2	25	0.053	0.059	81.27	0.010	5.08	0.201	0.634	0.111	38.90	8.46	1.00
31	166	5	29.4	25	0.052	0.061	81.27	0.010	5.08	0.201	0.677	0.128	33.88	9.50	1.00
32	6	5	21.1	40	0.077	0.101	81.27	0.013	5.08	0.260	0.683	0.162	38.94	9.30	1.00
33	145	5	27.2	80	0.157	0.131	81.27	0.010	5.08	0.201	0.542	0.089	31.50	7.25	1.00
34	96	5	27.2	90	0.202	0.200	81.27	0.010	5.08	0.201	0.416	0.076	29.83	7.67	0.95
35	131	5	30.0	90	0.199	0.285	81.27	0.010	5.08	0.201	0.409	0.088	20.40	7.40	1.00
36	126	5	27.2	90	0.202	0.315	81.27	0.010	5.08	0.201	0.437	0.079	23.40	8.20	1.00

Continued

Table 5.-- Continued.

File #	Burn #	Grp #	Temp C*	RH %	EMC (frac)	MC (frac)	Sigma (1/cm)	Beta	Depth (cm)	Load (kg)	R (m/min)	dw/dt (kg/min)	Fo (cm)	Fb (cm)	FI
37	36	6	31.7	11	0.024	0.023	81.27	0.010	10.16	0.402	0.938	0.346	85.78	18.23	1.00
38	51	6	30.0	11	0.023	0.025	81.27	0.010	10.16	0.402	1.020	0.384	80.78	15.95	1.00
39	63	6	27.2	25	0.053	0.055	81.27	0.010	10.16	0.402	0.911	0.340	80.86	20.14	1.00
40	61	6	27.2	25	0.053	0.057	81.27	0.010	10.16	0.402	0.871	0.329	86.47	19.88	1.00
41	173	6	27.2	65	0.117	0.098	81.27	0.010	10.16	0.402	0.777	0.300	63.38	12.18	1.00
42	148	6	27.2	80	0.157	0.142	81.27	0.010	10.16	0.402	0.706	0.241	55.13	12.13	1.00
43	102	6	27.2	90	0.202	0.219	81.27	0.010	10.16	0.402	0.569	0.210	43.14	11.00	1.00
44	127	6	27.2	90	0.202	0.297	81.27	0.010	10.16	0.402	0.505	0.181	43.63	12.75	1.00
45	45	7	27.2	9	0.021	0.014	81.27	0.010	20.32	0.804	1.270	0.934	164.68	36.79	1.00
46	62	7	27.2	25	0.053	0.058	81.27	0.010	20.32	0.804	1.088	0.791	167.64	35.80	1.00
47	172	7	27.2	65	0.117	0.109	81.27	0.010	20.32	0.804	0.957	0.715	162.48	31.94	1.00
48	147	7	27.2	80	0.157	0.140	81.27	0.010	20.32	0.801	0.891	0.656	111.93	24.00	1.00
49	202	7	27.2	80	0.157	0.205	81.27	0.010	20.32	0.804	0.368	0.695	90.00	29.00	1.00
50	206	7	27.2	95	0.236	0.236	81.27	0.010	20.32	0.804	0.711	0.523	90.83	19.67	1.00
51	128	7	27.2	90	0.202	0.297	81.27	0.010	20.32	0.804	0.564	0.470	57.38	21.25	0.70
52	163	0	29.4	9	0.020	0.016	81.27	0.022	1.27	0.110	0.467	0.041	10.43	6.71	0.90
53	47	8	27.2	9	0.021	0.017	81.27	0.020	2.54	0.201	0.731	0.134	36.24	10.25	1.00
54	42	8	29.4	11	0.023	0.026	81.27	0.020	2.54	0.201	0.637	0.117	41.21	7.98	1.00
55	35	8	31.7	0	0.010	0.028	81.27	0.020	2.54	0.201	0.691	0.122	62.28	15.38	1.00
56	64	8	27.2	25	0.053	0.055	81.27	0.020	2.54	0.201	0.594	0.104	37.59	11.00	1.00
57	63	8	27.2	25	0.053	0.056	81.27	0.020	2.54	0.201	0.574	0.118	44.79	13.67	1.00
58	57	8	27.2	25	0.053	0.056	81.27	0.020	2.54	0.201	0.648	0.119	39.20	9.25	1.00
59	2	8	22.0	40	0.077	0.072	81.27	0.026	2.54	0.260	0.639	0.123	37.79	9.11	1.00
60	5	8	21.1	40	0.076	0.102	81.27	0.026	2.54	0.260	0.571	0.136	29.39	11.28	1.00
61	150	8	27.2	80	0.157	0.141	81.27	0.020	2.54	0.201	0.423	0.072	22.96	8.29	1.00
62	94	8	27.2	90	0.202	0.209	81.27	0.020	2.54	0.201	0.346	0.064	34.30	10.03	0.90
63	123	8	27.0	90	0.202	0.278	81.27	0.020	2.54	0.201	0.324	0.060	15.75	8.31	0.70
64	1	0	21.1	40	0.077	0.085	81.27	0.026	5.08	0.521	0.698	0.332	42.65	18.23	1.00
65	162	0	29.4	9	0.020	0.019	81.27	0.022	20.32	1.773	1.289	2.089	300.00	68.58	1.00
66	46	9	27.2	9	0.021	0.017	81.27	0.040	1.27	0.201	0.713	0.131	40.43	10.03	1.00
67	71	9	27.2	25	0.053	0.055	81.27	0.040	1.27	0.201	0.459	0.080	36.99	14.98	0.90
68	174	9	27.2	65	0.117	0.103	81.27	0.040	1.27	0.201	0.269	0.049	9.51	6.71	0.60
69	149	9	27.2	80	0.157	0.143	81.27	0.040	1.27	0.201	0.386	0.062	24.50	8.13	1.00
70	101	9	27.2	90	0.202	0.212	81.27	0.040	1.27	0.201	0.170	0.031	7.75	6.50	0.50
71	130	9	29.4	90	0.200	0.256	81.27	0.040	1.27	0.201	0.166	0.031	4.50	6.56	0.50
72	43	10	26.7	9	0.021	0.039	81.27	0.040	2.54	0.402	0.642	0.242	56.76	16.54	1.00
73	69	10	27.2	25	0.053	0.059	81.27	0.040	2.54	0.402	0.464	0.175	51.96	18.83	1.00
74	72	10	20.0	25	0.054	0.068	81.27	0.040	2.54	0.402	0.525	0.209	63.79	18.67	1.00
75	4	10	21.1	40	0.077	0.107	81.27	0.052	2.54	0.521	0.574	0.242	41.99	13.33	1.00
76	151	10	27.2	80	0.157	0.140	81.27	0.040	2.54	0.402	0.479	0.165	36.67	10.33	1.00
77	100	10	27.2	90	0.202	0.205	81.27	0.040	2.54	0.402	0.372	0.155	33.63	17.13	0.90
78	125	10	27.2	90	0.202	0.296	81.27	0.040	2.54	0.402	0.284	0.094	27.71	14.43	0.90

Continued

Table 5.-- Continued.

File #	Burn #	Grp #	Temp C*	RH %	EMC (frac)	Mf (frac)	Sigma (1/cm)	Beta	Depth (cm)	Load (kg)	R (m/min)	dw/dt (kg/min)	FH (cm)	FD (cm)	FI
79	3	0	21.1	40	0.077	0.106	81.27	0.052	5.08	1.042	0.695	0.663	117.56	52.08	1.00
80	44	11	27.2	9	0.021	0.017	81.27	0.080	2.54	0.804	0.663	0.454	82.39	43.24	1.00
81	70	11	27.2	25	0.053	0.063	81.27	0.080	2.54	0.804	0.438	0.340	81.46	49.13	1.00
82	9	11	21.1	40	0.077	0.132	81.27	0.070	3.81	1.042	0.509	0.485	68.35	34.16	1.00
83	155	11	27.2	80	0.157	0.143	81.27	0.080	2.54	0.804	0.343	0.216	36.00	28.89	1.00
84	99	11	27.2	90	0.202	0.202	81.27	0.080	2.54	0.804	0.213	0.153	23.33	21.44	0.70
85	129	11	27.2	90	0.202	0.212	81.27	0.080	2.54	0.804	0.223	0.155	17.43	20.14	0.80
86	208	11	27.2	95	0.236	0.227	81.27	0.080	2.54	0.804	0.229	0.153	21.50	21.38	0.90
87	156	0	29.4	5	0.010	0.021	6.30	0.010	5.08	0.224	0.000	0.000	0.00	0.00	-0.60
88	54	12	32.0	12	0.023	0.026	6.30	0.010	20.32	0.895	0.159	0.137	19.10	14.89	1.00
89	81	12	27.2	25	0.053	0.058	6.30	0.010	20.32	0.895	0.093	0.076	21.33	10.17	0.80
90	180	12	27.2	65	0.117	0.112	6.43	0.010	20.32	0.895	0.000	0.000	0.00	0.00	-0.55
91	122	12	27.2	90	0.202	0.199	6.30	0.010	20.32	0.895	0.000	0.000	0.00	0.00	-0.90
92	204	13	31.7	15	0.034	0.010	6.30	0.020	5.08	0.448	0.046	0.017	8.00	4.63	0.40
93	31	13	29.4	15	0.035	0.026	6.30	0.020	5.08	0.448	0.042	0.018	5.83	4.42	0.50
94	74	13	27.2	25	0.053	0.057	6.30	0.020	5.08	0.448	0.000	0.000	0.00	0.00	-0.85
95	14	13	21.1	40	0.077	0.124	6.30	0.020	5.08	0.448	0.000	0.000	0.00	0.00	-0.80
96	26	14	29.4	10	0.023	0.026	6.30	0.020	10.16	0.895	0.098	0.081	21.64	10.57	0.70
97	80	14	27.2	25	0.053	0.059	6.30	0.020	10.16	0.895	0.065	0.050	17.33	7.50	0.70
98	18	14	21.1	40	0.077	0.114	6.30	0.020	10.16	0.895	0.043	0.035	6.50	5.69	0.50
99	195	14	27.2	85	0.177	0.179	6.30	0.020	10.16	0.895	0.000	0.000	0.00	0.00	-0.90
100	113	14	27.2	90	0.202	0.192	6.30	0.020	10.16	0.895	0.000	0.000	0.00	0.00	-0.80
101	159	15	27.2	5	0.013	0.025	6.30	0.020	20.32	1.790	0.329	0.510	69.00	29.13	1.00
102	169	15	29.4	25	0.052	0.068	6.30	0.020	20.32	1.790	0.179	0.292	40.67	19.39	1.00
103	179	15	27.2	65	0.117	0.113	6.43	0.020	20.32	1.790	0.116	0.203	27.36	13.17	1.00
104	200	15	27.2	85	0.177	0.176	6.30	0.020	20.32	1.790	0.065	0.104	18.88	11.50	1.00
105	117	15	27.2	90	0.202	0.217	6.30	0.020	20.32	1.790	0.065	0.130	27.25	10.25	0.50
106	142	15	27.2	90	0.202	0.238	6.30	0.020	20.32	1.790	0.070	0.115	10.00	10.13	0.70
107	210	15	27.2	95	0.236	0.283	6.30	0.020	20.32	1.790	0.000	0.000	0.00	0.00	-0.80
108	27	16	29.4	11	0.023	0.022	6.30	0.040	2.54	0.448	0.045	0.018	5.31	4.95	0.70
109	82	16	27.2	25	0.053	0.059	6.30	0.040	2.54	0.448	0.000	0.000	0.00	0.00	-0.80
110	17	16	21.1	40	0.077	0.119	6.30	0.040	2.54	0.448	0.000	0.000	0.00	0.00	-0.80
111	25	17	29.0	11	0.023	0.024	6.30	0.040	5.08	0.895	0.092	0.077	24.11	8.79	0.90
112	73	17	27.2	25	0.053	0.061	6.30	0.040	5.08	0.895	0.063	0.052	22.05	7.50	0.80
113	10	17	21.1	40	0.077	0.112	6.30	0.040	5.08	0.895	0.037	0.030	11.33	6.10	0.50
114	197	17	27.2	85	0.177	0.190	6.30	0.040	5.08	0.895	0.000	0.000	0.00	0.00	-0.95
115	115	17	27.2	90	0.202	0.193	6.30	0.040	5.08	0.895	0.000	0.000	0.00	0.00	-0.70

Continued

Table 5.-- Continued.

File #	Burn #	Grp #	Temp C*	RH %	EMC (frac)	Mf (frac)	Sigma (1/cm)	Beta	Depth (cm)	Load (kg)	R (m/min)	dw/dt (kg/min)	FH (cm)	FD (cm)	FI
116	158	18	27.2	5	0.013	0.020	6.30	0.040	10.16	1.790	0.250	0.409	56.88	20.88	1.00
117	77	18	27.2	25	0.053	0.058	6.30	0.040	10.16	1.790	0.232	0.380	88.00	19.86	1.00
118	16	18	21.1	40	0.077	0.122	6.30	0.040	10.16	1.790	0.116	0.193	39.82	14.47	1.00
119	199	18	27.2	85	0.177	0.175	6.30	0.040	10.16	1.790	0.060	0.110	16.13	8.63	1.00
120	114	18	27.2	90	0.202	0.200	6.30	0.040	10.16	1.790	0.059	0.091	21.00	10.38	0.90
121	144	18	27.2	90	0.202	0.243	6.30	0.040	10.16	1.790	0.053	0.083	9.88	8.75	0.80
122	211	18	27.2	95	0.236	0.276	6.29	0.040	10.16	1.790	0.000	0.000	0.00	0.00	-0.40
123	160	19	27.2	5	0.013	0.018	6.30	0.040	20.32	3.580	0.517	1.583	245.00	49.13	1.00
124	79	19	27.2	25	0.053	0.059	6.30	0.040	20.32	3.580	0.398	1.304	155.83	34.83	1.00
125	178	19	27.2	65	0.117	0.108	6.43	0.040	20.32	3.580	0.252	0.822	89.79	30.29	1.00
126	121	19	27.2	90	0.202	0.165	6.30	0.040	20.32	3.580	0.125	0.411	53.00	20.88	1.00
127	193	19	27.2	85	0.177	0.168	6.30	0.040	20.32	3.580	0.182	0.545	72.25	23.88	1.00
128	139	19	27.2	90	0.202	0.229	6.30	0.040	20.32	3.530	0.131	0.391	49.38	22.50	0.80
129	212	19	27.2	95	0.236	0.281	6.30	0.040	20.32	3.580	0.082	0.245	41.13	14.88	1.00
130	24	20	29.0	12	0.027	0.023	6.30	0.080	2.54	0.895	0.080	0.069	22.21	8.96	0.90
131	78	20	27.2	25	0.053	0.056	6.30	0.080	2.54	0.895	0.053	0.044	15.17	6.50	0.90
132	19	20	21.1	40	0.077	0.104	6.30	0.080	2.54	0.895	0.036	0.033	7.15	5.44	0.50
133	194	20	27.2	85	0.177	0.192	6.30	0.080	2.54	0.895	0.000	0.000	0.00	0.00	-0.95
134	116	20	27.2	90	0.202	0.209	6.30	0.080	2.54	0.895	0.000	0.000	0.00	0.00	-0.90
135	32	21	29.4	15	0.035	0.026	6.30	0.080	5.08	1.790	0.154	0.237	67.38	15.63	1.00
136	75	21	27.2	25	0.053	0.058	6.30	0.080	5.08	1.790	0.117	0.184	48.75	14.17	1.00
137	15	21	21.1	40	0.077	0.113	6.30	0.080	5.08	1.790	0.075	0.126	34.07	8.87	1.00
138	198	21	27.2	35	0.177	0.181	6.30	0.080	5.08	1.790	0.039	0.062	13.63	7.38	0.90
139	118	21	27.2	90	0.202	0.204	6.30	0.080	5.08	1.790	0.048	0.079	18.38	7.14	0.90
140	143	21	27.2	90	0.202	0.238	6.30	0.080	5.08	1.790	0.032	0.052	7.11	6.33	0.70
141	213	21	29.0	95	0.235	0.295	6.30	0.080	5.08	1.790	0.000	0.000	0.00	0.00	-0.90
142	157	22	27.2	5	0.013	0.016	6.30	0.160	2.54	1.790	0.084	0.140	30.13	11.50	1.00
143	168	22	29.4	25	0.052	0.065	6.30	0.160	2.54	1.790	0.056	0.090	25.53	7.85	1.00
144	176	22	27.2	65	0.117	0.109	6.43	0.160	2.54	1.790	0.038	0.063	20.46	5.16	0.90
145	119	22	27.2	90	0.202	0.163	6.30	0.160	2.54	1.790	0.022	0.037	7.89	4.89	0.50
146	196	22	27.2	85	0.177	0.206	6.30	0.160	2.54	1.790	0.023	0.035	8.86	4.86	0.70
147	140	22	27.2	90	0.202	0.237	6.30	0.160	2.54	1.790	0.000	0.000	0.00	0.00	-0.85
148	53	23	30.0	11	0.023	0.028	6.30	0.160	5.08	3.580	0.109	0.393	81.93	17.09	1.00
149	76	23	27.2	25	0.053	0.059	6.30	0.160	5.08	3.580	0.090	0.288	85.17	15.83	1.00
150	177	23	27.2	65	0.117	0.111	6.43	0.160	5.08	3.580	0.062	0.197	33.17	11.49	1.00
151	192	23	27.2	35	0.177	0.140	6.30	0.160	5.08	3.580	0.048	0.162	37.50	9.88	1.00
152	120	23	27.2	90	0.202	0.205	6.30	0.160	5.08	3.580	0.037	0.125	33.00	7.00	1.00
153	201	23	27.2	80	0.157	0.209	6.30	0.160	5.08	3.580	0.035	0.126	31.38	8.50	1.00
154	141	23	27.2	90	0.202	0.232	6.30	0.160	5.08	3.580	0.038	0.123	25.63	8.25	1.00
155	214	23	27.2	95	0.236	0.289	6.30	0.160	5.08	3.580	0.026	0.086	22.38	7.75	1.00

Continued

Table 5.-- Continued.

File #	Burn #	Grp #	Temp C*	RH %	EMC (frac)	Mf (frac)	Sigma (1/cm)	Beta	Depth (cm)	Load (kg)	R (m/min)	dw/dt (kg/min)	FH (cm)	FD (cm)	FI
156	164	0	29.4	9	0.020	0.019	3.15	0.010	10.16	0.448	0.000	0.000	0.00	0.00	-0.90
157	203	24	31.7	15	0.034	0.009	3.15	0.020	10.16	0.895	0.037	0.030	12.13	6.13	0.30
158	28	24	29.4	11	0.023	0.044	3.15	0.020	10.16	0.895	0.044	0.037	14.63	8.92	0.70
159	92	24	27.2	25	0.053	0.064	3.15	0.020	10.16	0.895	0.000	0.000	0.00	0.00	-0.70
160	30	25	29.4	15	0.035	0.025	3.15	0.040	10.16	1.790	0.083	0.138	25.73	16.82	0.90
161	85	25	27.2	25	0.053	0.061	3.15	0.040	10.16	1.790	0.038	0.059	11.38	10.83	0.80
162	11	25	21.1	40	0.077	0.059	3.15	0.040	10.16	1.790	0.000	0.000	0.00	0.00	-0.70
163	106	25	27.2	90	0.202	0.216	3.15	0.040	10.16	1.790	0.000	0.000	0.00	0.00	-0.90
164	56	26	29.5	11	0.023	0.025	3.15	0.040	20.32	3.580	0.389	1.331	189.30	101.58	1.00
165	90	26	27.2	25	0.053	0.066	3.15	0.040	20.32	3.580	0.215	0.705	69.50	46.63	1.00
166	21	26	21.1	40	0.077	0.136	3.15	0.040	20.32	3.580	0.104	0.350	45.43	34.64	1.00
167	185	26	27.2	75	0.053	0.160	3.15	0.040	20.32	3.580	0.042	0.148	10.88	15.25	0.80
168	105	26	27.2	90	0.202	0.203	3.15	0.040	20.32	3.580	0.033	0.107	9.13	15.75	0.25
169	137	26	27.2	90	0.202	0.261	3.15	0.040	20.32	3.580	0.000	0.000	0.00	0.00	-0.85
170	170	27	31.7	15	0.034	0.006	3.15	0.080	2.54	0.895	0.022	0.018	9.00	2.88	0.20
171	29	27	29.4	15	0.033	0.025	3.15	0.080	2.54	0.895	0.000	0.000	0.00	0.00	-0.70
172	87	27	27.2	25	0.053	0.061	3.15	0.080	2.54	0.895	0.000	0.000	0.00	0.00	-0.90
173	22	28	29.4	11	0.023	0.030	3.15	0.080	5.08	1.790	0.063	0.110	18.63	12.22	0.90
174	86	28	27.2	25	0.053	0.065	3.15	0.080	5.08	1.790	0.032	0.052	12.00	7.67	0.50
175	13	28	21.1	40	0.077	0.133	3.15	0.080	5.08	1.790	0.000	0.000	0.00	0.00	-0.80
176	104	28	27.2	90	0.202	0.221	3.15	0.080	5.08	1.790	0.000	0.000	0.00	0.00	-1.00
177	23	29	29.4	11	0.023	0.024	3.15	0.080	10.16	3.580	0.189	0.617	79.12	40.37	1.00
178	83	29	27.2	25	0.053	0.063	3.15	0.080	10.16	3.580	0.129	0.449	66.00	32.00	1.00
179	12	29	21.1	40	0.077	0.135	3.15	0.080	10.16	3.580	0.069	0.227	28.18	22.06	0.80
180	186	29	27.2	75	0.142	0.157	3.15	0.080	10.16	3.580	0.035	0.106	15.13	12.88	0.90
181	108	29	27.2	90	0.202	0.216	3.15	0.080	10.16	3.580	0.035	0.103	12.11	15.33	0.30
182	134	29	27.2	90	0.202	0.269	3.15	0.080	10.16	3.580	0.000	0.000	0.00	0.00	-0.90
183	34	30	29.4	10	0.023	0.023	3.15	0.080	20.32	7.161	0.420	2.750	326.74	97.86	1.00
184	89	30	27.2	25	0.053	0.058	3.15	0.080	20.32	7.161	0.308	2.017	208.66	61.40	1.00
185	93	30	27.2	25	0.053	0.061	3.15	0.080	20.32	7.161	0.295	1.932	240.98	62.00	1.00
186	181	30	27.2	65	0.117	0.117	3.11	0.080	20.32	7.161	0.168	0.968	100.82	48.72	1.00
187	188	30	27.2	75	0.142	0.154	3.15	0.080	20.32	7.161	0.141	0.837	146.37	36.25	1.00
188	135	30	27.2	90	0.202	0.204	3.15	0.080	20.32	7.161	0.063	0.394	36.13	26.38	1.00
189	109	30	27.2	90	0.202	0.210	3.15	0.080	20.32	7.161	0.112	0.673	62.38	30.13	1.00
190	207	30	27.2	95	0.236	0.245	3.15	0.080	20.32	7.161	0.072	0.394	55.50	32.75	1.00

Continued

Table 5.-- Continued.

File #	Burn #	Grp #	Temp C*	RH %	EMC (frac)	MF (frac)	Sigma (1/cm)	Beta	Depth (cm)	Load (kg)	F (m/min)	dw/dt (kg/min)	FH (cm)	FD (cm)	FI
191	55	31	33.0	12	0.023	0.026	3.15	0.160	5.08	3.580	0.100	0.327	63.68	26.37	1.00
192	84	31	27.2	25	0.053	0.067	3.15	0.160	5.08	3.530	0.077	0.245	38.14	23.64	1.00
193	20	31	21.1	40	0.077	0.160	3.15	0.160	5.08	3.580	0.033	0.106	24.20	11.83	0.80
194	187	31	27.2	75	0.053	0.171	3.15	0.160	5.08	3.580	0.021	0.073	11.13	10.13	0.80
195	110	31	27.2	90	0.202	0.214	3.15	0.160	5.08	3.580	0.000	0.000	0.00	0.00	-0.85
196	33	32	29.4	11	0.023	0.025	3.15	0.160	10.16	7.161	0.185	1.200	184.63	51.31	1.00
197	91	32	27.2	25	0.053	0.064	3.15	0.160	10.16	7.161	0.123	0.802	124.38	33.00	1.00
198	183	32	27.2	65	0.117	0.134	3.11	0.160	10.16	7.161	0.078	0.420	50.87	26.69	1.00
199	190	32	27.2	75	0.142	0.165	3.15	0.160	10.16	7.161	0.050	0.310	47.88	22.63	1.00
200	136	32	27.2	90	0.202	0.213	3.15	0.160	10.16	7.161	0.038	0.248	29.63	19.38	1.00
201	209	32	27.2	95	0.236	0.226	3.15	0.160	10.16	7.161	0.038	0.237	38.63	19.89	1.00
202	107	32	27.2	90	0.202	0.227	3.15	0.160	10.16	7.161	0.049	0.324	47.78	19.44	1.00
203	161	33	27.2	5	0.013	0.018	3.15	0.320	2.54	3.580	0.066	0.194	36.75	29.00	1.00
204	88	33	27.2	25	0.053	0.058	3.15	0.320	2.54	3.580	0.035	0.129	26.00	13.50	0.95
205	184	33	27.2	65	0.117	0.124	3.11	0.320	2.54	3.580	0.020	0.073	17.00	11.70	0.90
206	189	33	27.2	75	0.142	0.168	3.15	0.320	2.54	3.580	0.000	0.000	0.00	0.00	-0.40
207	111	33	27.2	90	0.202	0.202	3.15	0.320	2.54	3.580	0.000	0.000	0.00	0.00	-0.85
208	165	34	29.4	5	0.010	0.019	3.15	0.320	10.16	14.322	0.155	1.931	189.23	61.25	1.00
209	167	34	29.4	25	0.052	0.065	3.15	0.320	10.16	14.322	0.095	1.114	150.18	45.63	1.00
210	182	34	27.2	65	0.117	0.121	3.11	0.320	10.16	14.322	0.042	0.483	79.69	21.66	1.00
211	191	34	27.2	85	0.177	0.174	3.15	0.320	10.16	14.322	0.029	0.334	59.25	22.50	1.00
212	112	34	27.2	90	0.202	0.193	3.15	0.320	10.16	14.322	0.028	0.360	56.22	18.67	1.00
213	205	34	27.2	95	0.236	0.251	3.15	0.320	10.16	14.322	0.020	0.248	47.25	18.38	1.00
214	138	34	27.2	90	0.202	0.290	3.15	0.320	10.16	14.322	0.021	0.241	38.38	18.25	1.00

Table 6. -- Preliminary test fires.

File #	Burn #	Grp #	Temp C*	RH %	EMC (frac)	Mf (frac)	Sigma (1/cm)	Beta	Depth (cm)	Load (kg)	R (m/min)	dw/dt (kg/min)	FH (cm)	FD (cm)	FI
215	310	40	21.1	40	0.077	0.547	81.27	0.006	2.54	0.060	0.000	0.000	0.00	0.00	-0.90
216	307	40	21.1	40	0.077	0.423	81.27	0.006	7.62	0.181	0.253	0.042	16.30	5.70	0.90
217	307	40	21.1	40	0.077	0.524	81.27	0.006	7.62	0.181	0.000	0.000	0.00	0.00	-0.80
218	309	40	21.1	40	0.077	0.654	81.27	0.006	15.24	0.362	0.229	0.076	11.00	10.90	0.90
219	309	40	21.1	40	0.077	0.753	81.27	0.006	15.24	0.362	0.000	0.000	0.00	0.00	-0.80
220	305	40	21.1	40	0.077	0.329	81.27	0.020	2.54	0.201	0.223	0.041	15.00	10.16	0.90
221	305	40	21.1	40	0.077	0.520	81.27	0.021	2.54	0.211	0.000	0.000	0.00	0.00	-0.80
222	308	40	21.1	40	0.077	0.764	81.27	0.020	7.62	0.603	0.162	0.089	22.20	12.80	0.60
223	303	40	21.1	40	0.077	0.717	81.27	0.020	15.24	1.206	0.277	0.305	49.60	29.90	1.00
224	302	40	21.1	40	0.077	0.957	81.27	0.020	15.24	1.206	0.076	0.084	15.40	38.10	0.70
225	302	40	21.1	40	0.077	0.896	81.27	0.021	15.24	1.266	0.000	0.000	0.00	0.00	-0.70
226	311	40	21.1	40	0.077	0.560	81.27	0.040	2.54	0.402	0.000	0.000	0.00	0.00	-0.80
227	312	40	21.1	40	0.077	0.766	81.27	0.040	7.62	1.206	0.000	0.000	0.00	0.00	-0.70
228	313	40	21.1	40	0.077	1.190	81.27	0.040	15.24	2.412	0.000	0.000	0.00	0.00	-0.70
229	412	41	21.1	40	0.077	0.017	6.30	0.020	2.54	0.224	0.000	0.000	0.00	0.00	-0.75
230	413	41	21.1	40	0.077	0.118	6.30	0.020	7.68	0.677	0.000	0.000	0.00	0.00	-0.80
231	401	41	21.1	40	0.077	0.339	6.30	0.020	15.24	1.343	0.090	0.111	10.50	17.90	0.30
232	416	41	21.1	40	0.077	0.189	6.30	0.020	15.24	1.343	0.000	0.000	0.00	0.00	-0.65
233	407	41	21.1	40	0.077	0.059	6.30	0.040	2.54	0.448	0.022	0.009	6.00	4.30	0.50
234	404	41	21.1	40	0.077	0.241	6.30	0.040	2.54	0.448	0.000	0.000	0.00	0.00	-0.95
235	402	41	21.1	40	0.077	0.187	6.30	0.040	7.62	1.343	0.071	0.087	12.00	6.00	0.90
236	410	41	21.1	40	0.077	0.367	6.30	0.040	7.62	1.343	0.000	0.000	0.00	0.00	-0.95
237	409	41	21.1	40	0.077	0.463	6.30	0.040	15.24	2.685	0.053	0.130	23.90	7.80	0.90
238	405	41	21.1	40	0.077	0.211	6.30	0.080	2.54	0.895	0.000	0.000	0.00	0.00	-0.75
239	411	41	21.1	40	0.077	0.318	6.30	0.080	7.62	2.685	0.049	0.120	30.70	6.30	0.90
240	415	41	21.1	40	0.077	0.316	6.30	0.080	15.24	5.371	0.068	0.334	51.90	15.80	1.00
241	414	41	21.1	40	0.077	0.686	6.30	0.080	15.24	5.371	0.000	0.000	0.00	0.00	-0.95
242	419	42	21.1	40	0.077	0.037	3.15	0.040	7.62	1.343	0.041	0.050	9.60	11.00	0.20
243	419	42	21.1	40	0.077	0.037	3.10	0.040	7.62	1.343	0.000	0.000	0.00	0.00	-0.50
244	418	42	21.1	40	0.077	0.078	3.15	0.040	15.24	2.685	0.067	0.164	19.20	22.61	0.90
245	420	42	21.1	40	0.077	0.260	3.10	0.040	15.24	2.685	0.000	0.000	0.00	0.00	-0.50
246	426	42	21.1	40	0.077	0.113	3.10	0.080	2.54	0.895	0.000	0.000	0.00	0.00	-0.90
247	421	42	21.1	40	0.077	0.197	3.10	0.080	7.62	2.685	0.000	0.000	0.00	0.00	-0.70
248	424	42	21.1	40	0.077	0.313	3.15	0.080	15.24	5.371	0.030	0.147	24.30	16.70	0.90
249	424	42	21.1	40	0.077	0.400	3.10	0.080	15.26	5.378	0.000	0.000	0.00	0.00	-0.40
250	427	42	21.1	40	0.077	0.107	3.15	0.160	2.54	1.790	0.000	0.000	0.00	0.00	-0.80
251	428	42	21.1	40	0.077	0.107	3.15	0.160	3.81	2.685	0.026	0.064	12.50	8.40	0.70
252	422	42	21.1	40	0.077	0.241	3.15	0.160	7.62	5.371	0.025	0.125	13.80	9.60	0.95
253	423	42	21.1	40	0.077	0.299	3.15	0.160	7.62	5.371	0.017	0.083	13.10	9.10	0.60
254	423	42	21.1	40	0.077	0.363	3.15	0.160	7.62	5.371	0.000	0.000	0.00	0.00	-0.60
255	429	42	21.1	40	0.077	0.630	3.15	0.160	15.24	10.741	0.013	0.128	12.20	9.10	0.50
256	431	42	21.1	40	0.077	0.776	3.15	0.160	15.24	10.741	0.000	0.000	0.00	0.00	-0.70

Wilson, Ralph A.
1982. A reexamination of fire spread in free-burning porous fuel beds. USDA For. Serv. Res. Pap. INT-289, 28 p. Intermt. For. and Range Exp. Stn., Ogden, Utah 84401.

Experimental evidence from 250 test fires confirms the general formulation of Rothermel's 1972 mathematical model for predicting fire spread in wildland fuels. Numerical coefficients are reevaluated for the empirical relations governed by fuel bed geometry. Fuel moisture damping is functionally separated from extinction phenomena. Hypotheses are proposed that propagation flux is related to the optical density of the fuel bed; that the burning mass loss rate of different fuel size classes is proportional to fuel particle surface area; and that the marginal limit of self-sustained burning is dependent on the total fuel surface area in the bed as well as the fuel moisture content. Difficulties of measurement and physical interpretation of reaction intensities are discussed.

KEYWORDS: fire behavior, fire model, moisture damping, extinction, reaction intensity

The Intermountain Station, headquartered in Ogden, Utah, is one of eight regional experiment stations charged with providing scientific knowledge to help resource managers meet human needs and protect forest and range ecosystems.

The Intermountain Station includes the States of Montana, Idaho, Utah, Nevada, and western Wyoming. About 231 million acres, or 85 percent, of the land area in the Station territory are classified as forest and rangeland. These lands include grasslands, deserts, shrublands, alpine areas, and well-stocked forests. They supply fiber for forest industries; minerals for energy and industrial development; and water for domestic and industrial consumption. They also provide recreation opportunities for millions of visitors each year.

Field programs and research work units of the Station are maintained in:

Boise, Idaho

Bozeman, Montana (in cooperation with Montana State University)

Logan, Utah (in cooperation with Utah State University)

Missoula, Montana (in cooperation with the University of Montana)

Moscow, Idaho (in cooperation with the University of Idaho)

Provo, Utah (in cooperation with Brigham Young University)

Reno, Nevada (in cooperation with the University of Nevada)